Graphene and Graphene Oxide: Synthesis, Properties, and Applications

By *Yanwu Zhu, Shanthi Murali, Weiwei Cai, Xuesong Li, Ji Won Suk, Jeffrey R. Potts, and Rodney S. Ruoff**

There is intense interest in graphene in fields such as physics, chemistry, and materials science, among others. Interest in graphene's exceptional physical properties, chemical tunability, and potential for applications has generated thousands of publications and an accelerating pace of research, making review of such research timely. Here is an overview of the synthesis, properties, and applications of graphene and related materials (primarily, graphite oxide and its colloidal suspensions and materials made from them), from a materials science perspective.

1. Introduction

Graphene is an exciting material.[1] It has a large theoretical specific surface area (2630 m^{2}g^{-1}), high intrinsic mobility (200 000 cm^2 v^{-1} s^{-1}),[2,3] high Young's modulus (~1.0 TPa)[4] and thermal conductivity (~5000 Wm^{-1}K^{-1}),[5] and its optical transmittance (~97.7%) and good electrical conductivity merit attention for applications such as for transparent conductive electrodes,[6,7] among many other potential applications. Graphene has been experimentally studied for over 40 years,[8–14] and measurements of transport properties in micromechanically exfoliated layers,[15] of graphene grown on (SiC),[16] large-area graphene grown on copper (Cu) substrates,[17] as well as a variety of studies involving the use of chemically modified graphene (CMG) to make new materials,[18–21] have in part led to a surge in the number of publications and in the amount of, e.g., National Science Foundation grants recently awarded in the USA.[22]

As a robust yet flexible membrane, graphene provides essentially infinite possibilities for the modification or functionalization of its carbon backbone.[23] Graphite oxide (GO) offers potential for the production of CMG on the ton scale.[24] First prepared almost 150 years ago,[25] GO has emerged as a precursor offering the potential of cost-effective, large-scale production of graphene-based materials.[21]

In this review, the synthesis, physical properties, and potential applications of graphene and of CMG (with particular focus on graphene oxide) will be briefly discussed. Several recent reviews have appeared about graphene and related materials.[26–29] We also note reviews of the chemistry of GO or exfoliated platelets derived from GO, namely 'graphene oxide',[30] and of the chemistry of graphene.[31,32] Applications will be discussed for monolayer, bilayer and few-layer (3 to ~10 layers) graphene or GO-derived graphene-based materials.

2. Properties

2.1. Morphology and Structure

The graphene honeycomb lattice is composed of two equivalent sub-lattices of carbon atoms bonded together with σ bonds, as shown in **Figure 1a**. Each carbon atom in the lattice has a π orbital that contributes to a delocalized network of electrons. Whether freely suspended graphene has 'intrinsic' ripples or not has been addressed by Monte Carlo simulation[33] and transmission electron microscopy (TEM) studies.[34] The microscopic corrugations (Figure 1b) were estimated to have a lateral dimension of about 8 to 10 nm and a height displacement of about 0.7 to 1 nm. Sub-nanometer fluctuations in height for graphene platelets deposited on an SiO$_2$-on-Si substrate were studied by scanning tunneling microscopy (STM).[35] Although some STM experiments indicated a limited or negligible correlation between small (<0.5 nm in height) corrugations and local electrical properties,[36,37] evidence has been presented for strain induced local conductance modulations for bigger ripples (2–3 nm in height).[38,39] Ripples can be induced,[40] suggesting that the local electrical and optical properties of graphene could be altered through 'ripple-engineering' for possible application in devices.

Apart from 'intrinsic' corrugations, graphene in real 3D space can have other 'defects,' including topological defects (e.g., pentagons, heptagons, or their combination), vacancies, adatoms, edges/cracks, adsorbed impurities, and so on. Experiments have demonstrated that defects in a graphene layer found in the material containing single wall carbon nanotubes (CNTs), such as topological defects, vacancies, and adatoms, could be induced locally by electron irradiation and observed in TEM operating at 120 kV.[41] Graphene has been used as a TEM support membrane for the study of light atoms like carbon and hydrogen,[42] and Au nanoparticles.[43] Individual adatoms

[*] Dr. Y. Zhu, S. Murali, Dr. W. Cai, Dr. X. Li, J. W. Suk, J. R. Potts, Prof. R. S. Ruoff
Department of Mechanical Engineering and Texas Materials Institute
The University of Texas at Austin
One University Station C2200, Austin, TX 78712 (USA)
E-mail: r.ruoff@mail.utexas.edu

WILEY InterScience®
DISCOVER SOMETHING GREAT

REVIEW

on graphene, and carbon chains and vacancies, generated by knock-on by the electron beam in TEM (working at 100 kV) could be investigated dynamically, providing insights into generation of defects and their evolution.[42] Atomic resolution imaging of graphene has been achieved in TEM using an aberration-correction technique in combination with a monochromator; point defects, formation and annealing of Stone-Wales defects, and multiple pentagons/heptagons combinations were observed *in situ*.[44] The stability and dynamics of the edge of a hole in a suspended graphene platelet has been studied; TEM images with a stated sub-Ångstrom resolution showed that both 'armchair' and 'zigzag' configurations could be formed during the edge reconstruction and 'zigzag' edges were observed to be particularly stable under electron irradiation at 80 kV acceleration voltage.[45] Edge-reconstruction was achieved by Joule heating inside a TEM-STM system, yielding sharp zigzag and armchair edges in graphene ribbons.[46]

2.2. Electronic Properties

As a consequence of the graphene structure, the first Brillouin zone has two inequivalent points K and K' (called Dirac points), where a band crossing occurs (Figure 1a). The tight-binding approach considering only the first nearest neighbor interaction provides the dispersion relation of the electrons near the K/K' points:[47,48]

$$E_\pm(\vec{k}) = \pm t \sqrt{1 + 4\cos\frac{\sqrt{3}k_x a}{2}\cos\frac{k_y a}{2} + 4\cos^2\frac{k_y a}{2}} \qquad (1)$$

where $a = \sqrt{3}a_{CC}$, a_{CC} is the carbon-carbon bonding length (0.142 nm), and t, the transfer integral, is the nearest neighbor hopping energy with a magnitude of about 2.8 eV. The minus sign applies to the valence (π) band that is fully occupied in graphene, and the plus sign corresponds to the empty conduction (π^*) band. By expanding Equation (1) near the K/K' points, the dispersion can be obtained as

$$E_\pm(\vec{q}) \approx \pm \hbar v_F |\vec{q}| \qquad (2)$$

where $\vec{q}$ is the momentum measured relative to the Dirac point; $\hbar = h/2\pi$, where h is Planck's constant; and v_F is the Fermi velocity, given by $v_F = \sqrt{3}ta/2$, with a value of about 1×10^6 ms^{-1}. The linear band structure closely resembles the Dirac spectrum for massless fermions.[1] The electronic states near Dirac points are composed of states belonging to the different sub-lattices, and their relative contributions have to be taken into account by using two-component wave functions. Thus, the effective Hamiltonian near K/K' can be expressed by the Dirac equation with zero mass:

$$\hat{H} = \hbar v_F \begin{pmatrix} 0 & k_x - ik_y \\ k_x + ik_y & 0 \end{pmatrix} = \hbar v_F \, \vec{\sigma} \cdot \vec{k} \qquad (3)$$

where $\vec{k}$ is the momentum of the quasi-particles in graphene and $\vec{\sigma}$ is the 2D Pauli matrix. The two-component description of graphene is similar to the spinor wave function in quantum electrodynamics (QED), but the 'spin' index for graphene

Yanwu Zhu is a postdoctoral fellow in the Ruoff group at The University of Texas at Austin. He received his M.S. (2003) from Peking University (China) and Ph.D. (2007) from the National University of Singapore (NUS), both in Physics. He worked as a research fellow in the NUS Nanoscience & Nanotechnology Initiative, Singapore prior to his move to UT Austin. His research includes the synthesis and processing of metal oxide nanostructures and graphene materials and study of their use in electrochemical energy storage.

Shanthi Murali is currently pursuing a Ph.D. in Materials Science and Engineering at The University of Texas at Austin under the direction of Prof. Rodney S. Ruoff. She received her M.S. degree in Chemical Engineering from Auburn University in 2008, where her thesis work consisted of liquid crystalline assembly of nanowires. Her current research studies of chemically modified graphene materials, especially for use in electrochemical energy storage.

Rod Ruoff holds the Cockrell Family Regents Chair at The University of Texas at Austin, after having been Director of the Biologically Inspired Materials Institute at Northwestern University. He received his BS in Chemistry from UT-Austin and Ph.D. in Chemical Physics from the University of Illinois-Urbana (advisor H.S. Gutowsky). Prior to Northwestern he was a Staff Scientist at the Molecular Physics Laboratory, SRI International and then Associate Professor of Physics at Washington University. He is a co-founder of Graphene Energy Inc., founder of Nanode, Inc., and author of 225 refereed articles in materials science, physics, mechanics, chemistry, electrochemical energy storage, and biomedical research.

indicates the sub-lattice rather than the real spin of the electrons, and is usually referred to as 'pseudospin.'

Experimental observation of the cyclotron mass dependence on the square root of the electronic density in graphene was

Materials
Views
www.MaterialsViews.com

ADVANCED
MATERIALS
www.advmat.de

REVIEW
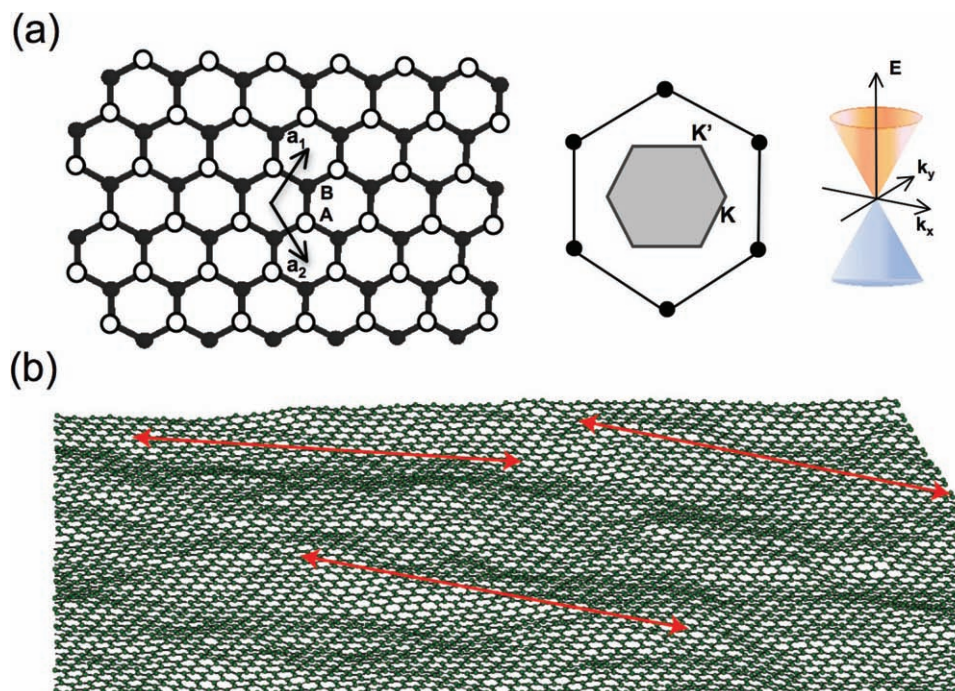
Figure 1. (a) Schematics of the crystal structure, Brillouin zone and dispersion spectrum of graphene; (b) 'Rippled graphene' from a Monte Carlo simulation. The red arrows are ~8 nm long. Reproduced with permission from[33] (b). Copyright: 2007 Nature Publishing Group (b).

interpreted as evidence for the existence of massless Dirac quasiparticles in graphene.[49,50] As a zero band gap semiconductor, graphene displays an ambipolar electric field effect and charge carriers can be tuned continuously between electrons and holes in concentrations as high as 10^{13} cm^{-2}, with room temperature mobilities of up to 15 000 cm^{2}V^{-1}s^{-1} (**Figure 2a**).[15,49,50]

Moreover, the observed mobilities depend weakly on temperature, suggesting that an ultrahigh mobility could be realized in graphene at room temperature.[3] By minimizing impurity scattering, mobilities in excess of 200 000 cm^{2}V^{-1}s^{-1} were achieved in suspended graphene,[2] an exceptionally high value.[51] The mobility in graphene remains high even at high carrier density
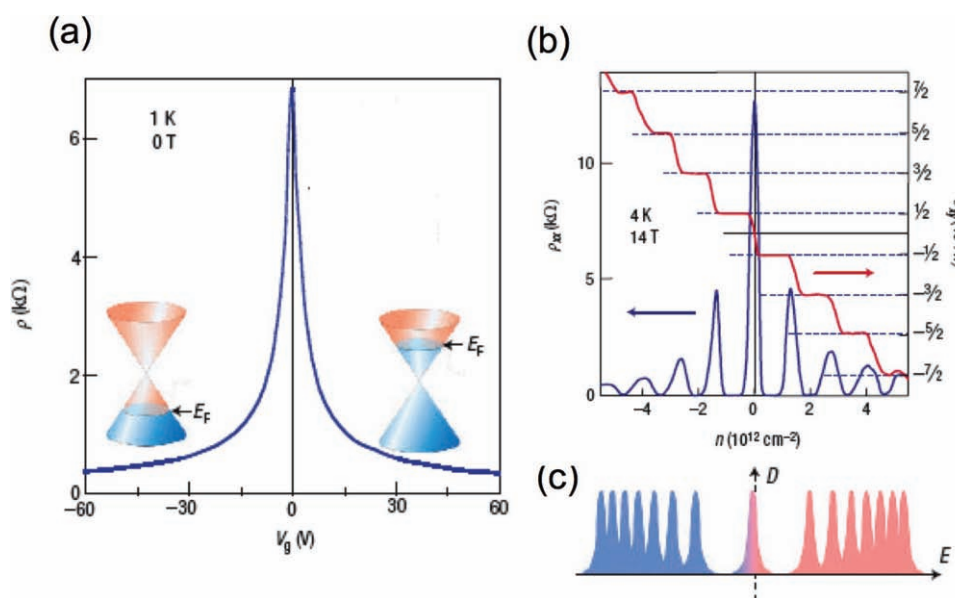
Figure 2. (a) Ambipolar electric field effect in monolayer graphene. The insets show the changes in the position of the Fermi energy E_F with changing gate voltage V_g; (b) The hallmark of massless Dirac fermions is QHE plateau in σ_{xy} at half integers of $4e^2/h$; (c) Landau levels in the density of states D in graphene are described by $E_N \propto \sqrt{N}$ for massless Dirac fermions. Reproduced with permission from[1] (a and c) and[49] (b). Copyright: 2007 Nature Publishing Group (a and c) and 2005 Nature Publishing Group (b).

WILEY
InterScience®
DISCOVER SOMETHING GREAT
3

REVIEW

in both electrically and chemically doped devices,[52] displaying evidence of ballistic transport on the sub-micrometer scale.[53] Another measure of the electronic quality of graphene is whether the quantum Hall effect (QHE) can be observed at room temperature.[54]

The "half-integer" QHE observed in graphene (Figure 2b), with the Hall conductivity expressed as $\sigma_{xy} = \pm 4e^2/h(N + 1/2)$ where N is the Landau level index,[49] can be understood based on the massless Dirac fermions in graphene. The energy quantization of the graphene electronic structure in a magnetic field with a field strength B is described by $E_N = \pm v_F \sqrt{2e\hbar BN}$ where ± refers to electrons and holes.[55,56] Of particular importance is the existence of a zero-energy state at $N = 0$ (as shown in Figure 2c), which is shared by electrons and holes, leading to the QHE in graphene. From STM studies on graphene grown on SiC, the discrete, non-equally-spaced Landau level spectrum, including the hallmark zero-energy state of graphene, was observed.[57] While the picture of non-interacting Dirac fermions apparently is appropriate for graphene at low energy excitations,[48] strong interactions and collective effects have been predicted near the Dirac points.[58,59] Recently, the experimental observation of the 'fractional QHE' (FQHE) from high-quality, suspended graphene with a two-probe measurement geometry was reported.[60,61] It was stated that the FQHE is quite robust, appearing at low temperatures (e.g., 1.2 K) in a field as low as 2 T and a temperature persisting up to 20 K in a field of 12 T.[60] The suppression of weak localization,[62] the existence of finite minimal conductivity (e^2/h per carrier type),[49,63] and Klein tunneling in graphene p-n junctions,[64] are mentioned as reasons why graphene offers opportunities for the testing of QED effects.

2.3. Mechanical Properties

The mechanical properties of monolayer graphene including the Young's modulus and fracture strength have been investigated by numerical simulations such as molecular dynamics.[65–67] The Young's modulus of few-layer graphene was experimentally investigated with force-displacement measurements by atomic force microscopy (AFM) on a strip of graphene suspended over trenches.[68] Circular membranes of few-layer graphene were also characterized by force-volume measurements in AFM.[69] Recently, the elastic properties and intrinsic breaking strength of free-standing monolayer graphene were measured by nanoindentation using an AFM (**Figure 3a** and b).[4] It was reported that defect-free graphene has a Young's modulus of 1.0 TPa and a fracture strength of 130 GPa. CMG was also investigated by a similar AFM indentation method.[70] The CMG obtained by reducing graphene oxide with a hydrogen plasma exhibited a mean elastic modulus of 0.25 TPa with a standard deviation of 0.15 TPa; the fracture strength was not reported.

A 'paper-like' material (Figures 3c and d) made by flow-directed assembly of individual graphene oxide platelets has been reported.[20] The average elastic modulus and the highest fracture strength obtained were ~32 GPa and ~120 MPa, respectively. The mechanical properties of this 'graphene oxide paper' were improved by introducing chemical cross-linking between individual platelets using divalent ions[71] and polyallylamine.[72] Instead of preparation by filtration, a self-assembled graphene oxide paper was made at a liquid/air interface by evaporating the hydrosol of graphene oxide.[73] This self-assembled paper showed a slightly lower modulus but similar tensile strength as compared with those prepared by filtration. In addition, a paper composed of stacked and overlapped reduced graphene oxide platelets was obtained by controlled reduction of graphene oxide dispersions with hydrazine.[74] After annealing, its stiffness and tensile strength were higher than those of graphene oxide papers reported to date.

2.4. Optical Properties

The high-frequency conductivity for Dirac fermions in graphene has been stated to be a constant equal to $\pi e^2/2h$, from the infrared through the visible range of the spectrum.[56,75] The optical transmittance T and reflectance R are then $T = (1 + 1/2\pi\alpha)^{-2}$ and $R = 1/4\pi^2\alpha^2 T$ for normal incidence light (where $\alpha = 2\pi e^2/hc \approx 1/137$, e is the electron charge, c the light speed, and h Planck's constant); the opacity is $(1 - T) \approx \pi\alpha \approx 2.3\%$. The expression of T and R in terms of fundamental constants that do not directly involve material parameters is stated to be a
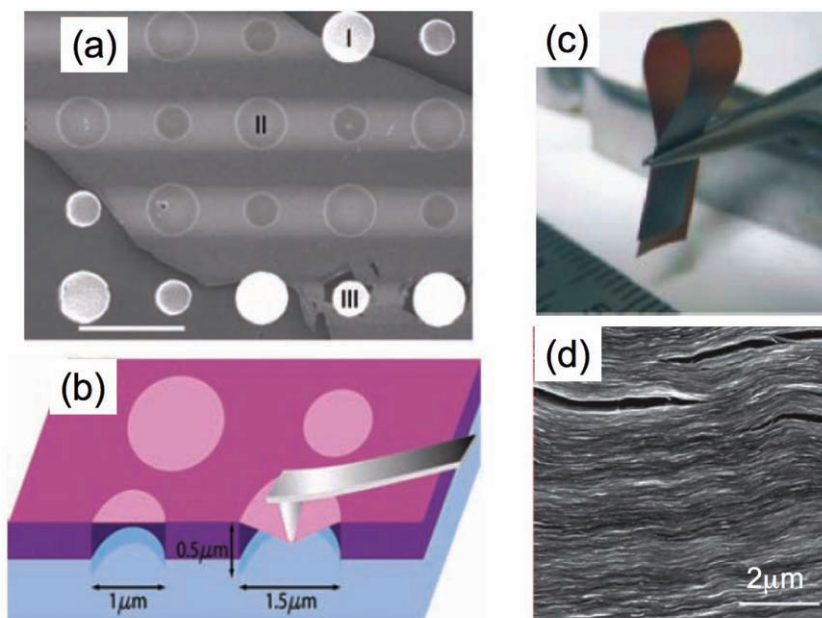
Figure 3. (a) Scanning electron microscopy (SEM) image of a graphene flake spanning an array of circular holes (scale bar, 3μm) and (b) Schematic illustration of nanoindentation on membranes; (c) and (d) show graphene oxide paper and its cross-section in SEM. Reproduced with permission from[4] (a and b) and[20] (c and d). Copyright: 2008 American Association for the Advancement of Science (a and b) and 2007 Nature Publishing Group (c and d).
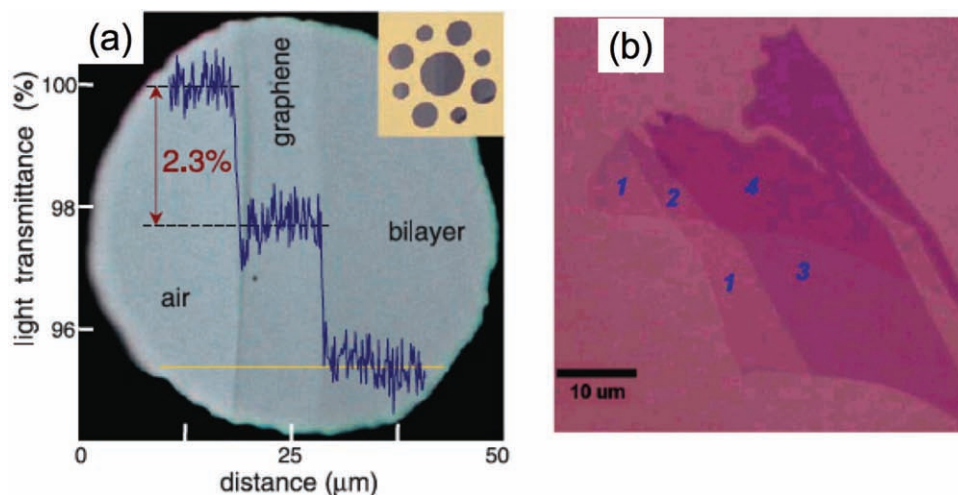
Figure 4. (a) Photograph of a 50-μm aperture partially covered by graphene and its bilayer. The line scan profile shows the intensity of transmitted white light along the yellow line. Inset shows the sample design: a 20-μm thick metal support structure has apertures 20, 30, and 50 μm in diameter with graphene flakes deposited over them; (b) Optical image of graphene flakes with one, two, three, and four layers on a 285-nm thick SiO₂-on-Si substrate. Reproduced with permission from[77] (a) and[84] (b). Copyright: 2008 American Association for the Advancement of Science (a) and 2007 American Chemistry Society (b).

result of the structure and electronic properties of graphene.[76] As shown in **Figure 4a**, this constant transparency (~97.7%) has been experimentally observed for graphene in the visible range and the transmittance linearly decreases with the number of layers for n-layer graphene.[77] A deviation from this 'universal behavior' has been found for incident photons with energy lower than 0.5 eV, which was attributed to the finite temperature and a doping-induced chemical potential shift of the charge-neutrality (Dirac) point.[78]

Inter-band optical transitions in graphene have been probed by infrared spectroscopy, and gate-dependent optical transitions have been reported.[79] Due to the low density of states near the Dirac point in graphene, a shift of the Fermi level due to the gate causes a significant variation of charge density, leading to a significant change in transmission. The relaxation and recombination of photo-generated electron-hole pairs in graphene occurs on a timescale of tens of picoseconds, depending on the carrier concentration of graphene.[80,81] Given the high carrier transport velocity even under a moderate electrical field, an ultrafast (up to 40 GHz) and efficient (6–16% internal quantum efficiency) photoresponse has been observed for graphene field effect transistors (FET),[82] suggesting graphene-based high-speed optoelectronic devices for communications, detection, sensing, and so on.

Given the low throughput of AFM, STM, TEM, and methods for characterizing the transport properties of graphene, other methods are needed to rapidly locate graphene, to identify its morphology and quality and to distinguish the number of layers (n) in n-layer graphene. The optical contrast of graphene on various substrates such as SiO₂/Si,[83–85] Si₃N₄/Si,[86] SiC,[87] Al₂O₃/Si[88] has been studied. The insulator layer thicknesses employed for the observation of graphene on SiO₂/Si include 90,[83] 280,[83] 300,[89] 465[85] nm; for Si₃N₄/Si 68 nm,[86] and for Al₂O₃/Si, 72 nm.[88] The contrast of graphene on such substrates

is dependent on the wavelength[83] and the incident angle[90] of the illumination. The thickness of n-layer graphene with less than 10 layers has been determined using white light illumination on samples supported on a 285 nm SiO₂/Si substrate (Figure 4b).[84] The refractive index of monolayer graphene was obtained as $n = 2.0 - 1.1i$ in the visible range,[84] slightly different from that of bulk graphite $n = 2.6 - 1.3i$.[91] Another study argued that the complex refractive index of graphene and graphite could be generally expressed as $n = 3 - iC/(3\lambda)$ (where $C = 5.446$ μm⁻¹ and λ is wavelength), by fitting to experimental spectra as a function of wavelength.[92]

2.5. Raman Spectroscopy of Graphene

Raman spectroscopy has been used to characterize graphene and several review articles have been published discussing the optical phonon spectrum and Raman spectrum of graphene.[93–96] The Raman spectra of graphene includes the G peak located at ~1580 cm⁻¹ and 2D peak at ~2700 cm⁻¹, caused by the in-plane optical vibration (degenerate zone center E_{2g} mode) and second-order zone boundary phonons, respectively. The D peak, located at ~1350 cm⁻¹ due to first-order zone boundary phonons, is absent from defect-free graphene, but exists in defected graphene. It was proposed that Raman could be used to distinguish the 'quality' of graphene and to determine the number of layers for n-layer graphene (for n up to 5) by the shape, width, and position of the 2D peak.[97] As shown in **Figure 5**, the 2D peak shifts to higher wavenumber values and becomes broader for an increasing number of layers.

The shifting and splitting of Raman modes can be used to analyze mechanical strain in graphene. For example, Raman spectra of epitaxial graphene grown on SiC show a significant phonon 'hardening' (blue shift of the G and 2D peaks), mainly due to the
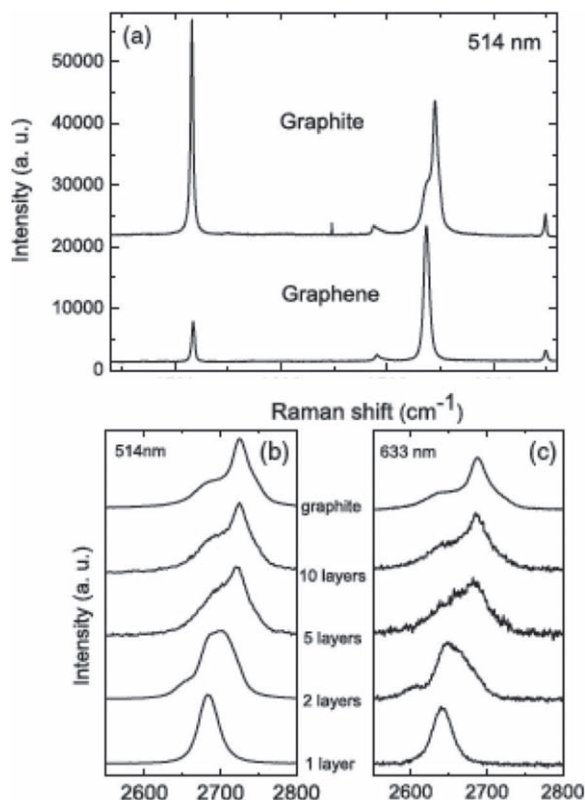
Figure 5. (a) Comparison of Raman spectra at 514 nm for bulk graphite and graphene. They are scaled to have similar height of the 2D peak at 2700 cm^{-1}; (b) Evolution of the spectra at 514 nm with the number of layers; (c) Evolution of the Raman spectra at 633 nm with the number of layers. Reproduced with permission from.[97] Copyright: 2006 American Physics Society.

compressive strain that occurs when the sample is cooled down after growth.[98,99] It has been stated that the substrates play a negligible role in the Raman spectrum of micromechanically cleaved graphene transferred onto them, indicating the weak interactions between the transferred graphene and such substrates.[100] The frequency of the G and 2D peaks can also be tuned by charge doping through electron-phonon coupling changes.[101,102] The Raman spectral signatures of epitaxial graphene grown on SiC, especially the width of the 2D peak, have been correlated to the carrier mobility of the graphene.[103] The intensity ratio of the D and G peak has been used as a metric of disorder in graphene, such as arising from ripples, edges, charged impurities, presence of domain boundaries, and others.[93] For edges, the intensity of the D peak depends on the edge structure; it is weak at the zigzag edge and strong at the armchair edge.[104,105]

2.6. Thermal Properties

Since the carrier density of non-doped graphene is relatively low, the electronic contribution to thermal conductivity (Wiedemann-Franz law) is negligible. The thermal conductivity (κ) of graphene is thus dominated by phonon transport, namely diffusive conduction at high temperature and ballistic conduction at sufficiently low temperature.[106]

MD simulations[107] based on the Green-Kubo approach have shown a $\kappa \propto 1/T$ dependence for defect-free graphene as temperature T increases beyond about 100 K. A room temperature thermal conductivity of about 6000 $Wm^{-1}K^{-1}$ for a suspended monolayer graphene was predicted, and this value was stated to be much higher than that of graphitic carbon.[107] A calculation based on the Boltzmann equation predicts a particular dependence of κ on the width d of GNRs and on the 'roughness' of the edges, when the diffusive conduction dominates κ.[108] Non-equilibrium MD was used to investigate the κ of GNRs with different edge shapes as a function of length, width, and strain.[109] It was found that κ follows a power law dependence on the length L of GNRs ($\kappa \propto L^\beta$), where β varies from 0.3 to 0.5 at room temperature. It was stated that the strong length dependence of thermal conductivity on L may indicate very long phonon mean free paths in GNRs.

In a recent optical measurement using the shift in the Raman G band, a thermal conductivity value of about 5000 $Wm^{-1}K^{-1}$ was obtained for a suspended monolayer graphene 'flake', produced by using mechanical exfoliation.[5,110] As shown in **Figure 6a**, a trench was used to suspend the graphene. A laser beam was focused on the center of the suspended graphene. The heat flowed radially from the center of the graphene to the support. The heat loss via air was stated to be negligible compared to heat conduction in the graphene.[111] The temperature rise in the heated graphene causes a red-shift of the Raman G peak because of bond softening. The red-shift of the G peak of graphene linearly depends on the sample temperature at relatively low laser power.[112] The frequency of the Raman G peak was measured as a function of excitation power (Figure 6b), where the thermal conductivity, as high as ~5000 $Wm^{-1}K^{-1}$, was extracted from the slope of the trend line. In another study, a thermal conductivity of ~2500 $Wm^{-1}K^{-1}$ (at 350 K) was obtained from chemical vapor deposition (CVD) grown graphene deposited onto a thin silicon nitride membrane having an array of through-holes; the silicon nitride was coated with a thin layer of gold for better thermal contact.[113] It has been recently reported[114] that the thermal conductivity of micromechanically exfoliated graphene deposited on a SiO_2 substrate is about 600 $Wm^{-1}K^{-1}$ (Figure 6c and d), exceeding those of metals like Cu. This value, lower than values obtained to date for suspended grapheme (whether micromechanically exfoliated[5] or CVD grown[113]) was attributed to the phonons leaking across the graphene-support interface and strong interface scattering of flexural modes.[114]

3. Applications

3.1. Field Effect Transistors

Due to the unique band structure, the carriers in graphene are bipolar, with electrons and holes that can be continuously tuned by a gate electrical field.[15] Graphene FET devices with a single back gate have been investigated by several groups (among many).[15,49,50,115] Experimental values of the field-effect mobility of graphene are one order of magnitude higher than
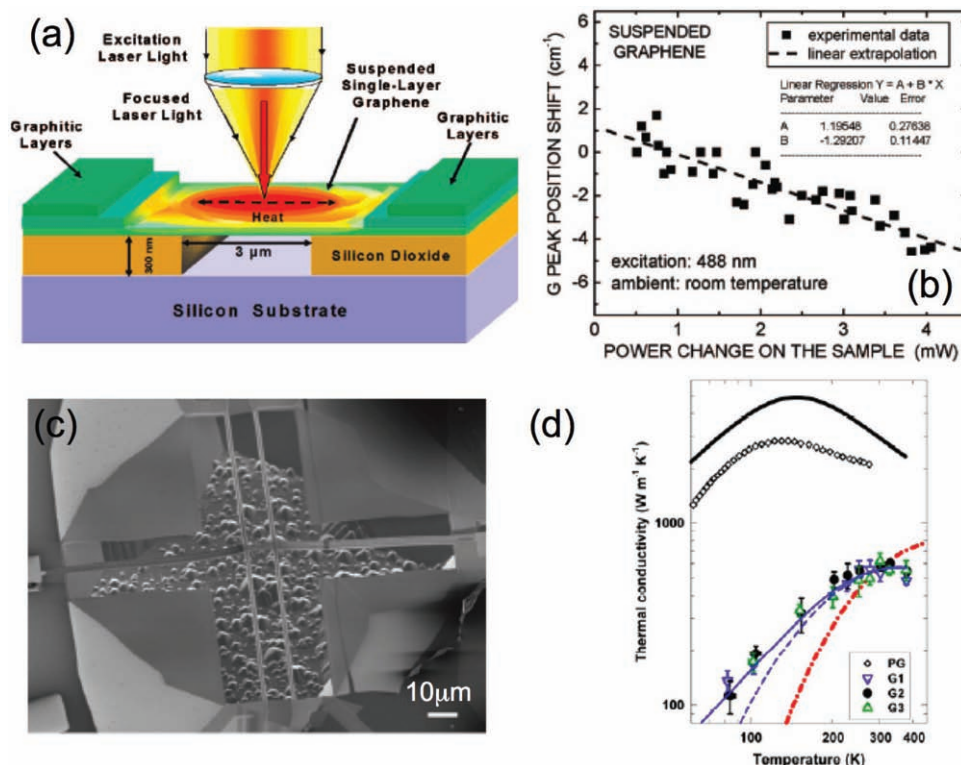
Figure 6. (a) Schematic of an experiment showing the excitation laser light focused on a graphene flake suspended across a trench. The focused laser light creates a local hot spot and generates a heat wave inside graphene propagating toward heat sinks; (b) Shift in Raman G peak position versus change in total dissipated power. The sample was excited at 488 nm and spectra were recorded at room temperature in the backscattering configuration. (c) SEM image of the suspended device for the thermal conductivity measurement of graphene. (d) Measured thermal conductivity values of graphene devices G1, G2, and G3, the highest reported values of pyrolytic graphite (PG), along with the Boltzmann transport equation (BTE) calculation results of suspended graphene (thick black solid line) and supported graphene (thin blue solid line and blue dashed line), as well as the relaxation time approximation (RTA) calculation result (thick red dash-dot line) for supported graphene. Specular edges are assumed in the calculations. Reproduced with permission from[5] (a and b) and[114] (c and d). Copyright: 2008 American Physics Society (a and b) and 2010 American Association for the Advancement of Science (c and d).

that of Si. Batch fabrication of graphene transistors on the basis of graphene grown on Cu films has been proposed as a method to achieve large-scale transistor arrays with uniform electrical properties.[116] A high frequency graphene FET operating at a frequency up to 26 GHz has been reported using top gate geometry.[117] With use of an organic polymer buffer layer between graphene and conventional gate dielectrics, the device mobility was further optimized,[118] and a cutoff frequency of 100 GHz has been reported based on epitaxial graphene formed on a 2-inch SiC wafer.[119] A single electron transistor (SET), based on graphene quantum dots made by electron beam lithography (EBL) (**Figure 7**), has been reported.[120] It was reported that such graphene SETs behave like conventional larger size SETs, exhibiting periodic Coulomb blockade peaks; for quantum dots smaller than 100 nm, the peaks become strongly non-periodic, and this was attributed to a major contribution of quantum confinement and described by 'the chaotic neutrino billiards'.[120]

Due to the finite minimum conductance of graphene at zero gate voltage, relatively low I_{on}/I_{off} ratios (e.g., 100[15]) have been reported from FET devices made from pristine graphene. Several routes have been developed to induce and control an energy gap in graphene for shutting off the current. For

example, graphene epitaxially grown on a SiC substrate could have a band splitting of up to 0.26 eV, due to the interaction with the substrate.[121] Angle-resolved photoemission spectroscopy (ARPES) studies[121] suggested that this gap decreased as the sample thickness increased and eventually approached zero when the number of layers exceeded four. On the other hand, an insulating state can be created in bilayer graphene FETs by using an additional top gate in addition to the global back gate.[122] At low temperatures, a small gap (10 meV) was opened in the presence of a perpendicular electric field. Using a similar double-gated structure and infrared microspectroscopy, a gate-controlled, continuously tunable band gap of up to 0.25 eV in bilayer graphene FETs was observed at room temperature.[123]

An alternative approach to introduce a band gap in graphene is to constrict its lateral dimensions to generate quasi one-dimensional (1D) GNRs. Similar to the situation in single walled CNTs, the confinement gap (ΔE) in GNRs is expected to scale inversely with the ribbon width (W) as $\Delta E = 2\pi \hbar v_F / 3 W$.[124,125] EBL patterning, coupled with oxygen plasma etching, has been used to fabricate GNR FETs with widths between 10 and 100 nm; a band gap of 0.2 eV was observed from a ribbon with a width of 15 nm.[126] Using similar devices, I_{on}/I_{off} ratios of up
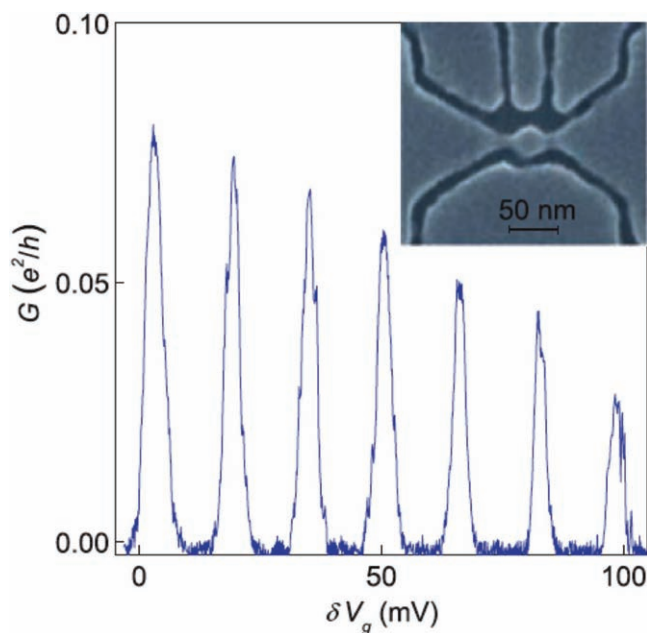
Figure 7. A graphene-based SET. Conductance G of a device with the central island of 250 nm in diameter and distant side gates as a function of V_g in the vicinity of +15 V; $T = 0.3$ K. The inset shows one of the smaller devices illustrating the high resolution lithography "that allows features down to 10 nm". Reproduced with permission from[120] Copyright: 2008 American Association for the Advancement of Science.

to 10^4 have been reported.[127] A chemical route has been developed to produce GNRs with widths below 10 nm (**Figure 8**).[128] The procedure involved sonication of thermally exfoliated graphite in an organic solution of a π-conjugated organic polymer. The energy gap from the narrowest ribbons ($W = 2$ nm) was estimated to be 0.4 eV and I_{on}/I_{off} ratios of up to 10^7 were obtained from the GNR based FETs.[128] Preparation of GNRs from 'unzipped' CNTs using plasma etching[129] or chemical oxidization,[130] are potential production methods for future graphene FETs.

The bipolar feature of graphene makes its carrier type and concentration sensitive to doping, electrically and/or chemically. A graphene p-n junction has been prepared in which carrier type and density in two adjacent regions were locally controlled by electrostatic gating.[131] A fractional conductance quantization in the bipolar regime has been observed experimentally[131] and explained by theory.[132] Furthermore, theory has predicted that a graphene p-n junction may be used to focus electrons, for turning the n-p-n junction into a Veselago lens.[133] Graphene p-n-p junctions with contactless, suspended top gates have been reported.[134] Graphene is usually p-doped due to adsorbates like H_2O. Preparation of n-doped graphene materials by high-power electrical annealing of GNRs[135] or high temperature annealing of graphene oxide[136] in ammonia (NH_3) has been demonstrated. A p-type GNR FET was obtained with an I_{on}/I_{off} ratio of about 10^5 after annealing.[135] Electrochemical doping, realized by adding an electrochemical top-gate on the graphene FET, has been reported and a doping level of up to 5×10^{13} cm^{-2}
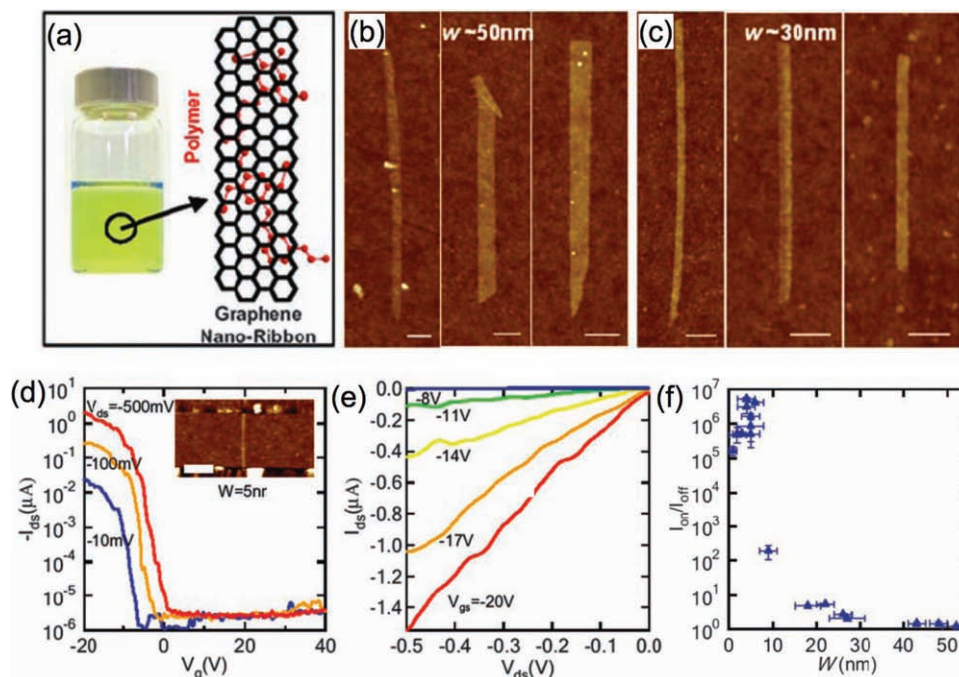
Figure 8. (a) (Left) Photograph of a polymer poly(m-phenylenevinylene-co-2,5-dioctoxy-p-phenylenevinylene) (pmPV)/1,2-dichloroethane(DCE) solution with GNRs stably suspended in the solution. (Right) Schematic drawing of a graphene nanoribbon with two units of a PmPV polymer chain adsorbed on top of the graphene via π stacking; (b and c) AFM images of selected GNRs with 50 nm and 30 nm widths, respectively; (d) Transfer characteristics for a GNR of w ≈ 5 nm (thickness ~ 1.5 nm, ~two layers) and channel length L ≈ 210 nm with Pd contacts. (Inset) The AFM image of this device. Scale bar is 100 nm; (e) I_{ds}-V_{ds} characteristics recorded under various V_{gs} for the device in (d); (f) Measured I_{on}/I_{off} ratios (under $V_{ds} = 0.5$ V) for GNRs of various ribbon widths. Reproduced with permission from.[128] Copyright: 2008 American Association for the Advancement of Science.
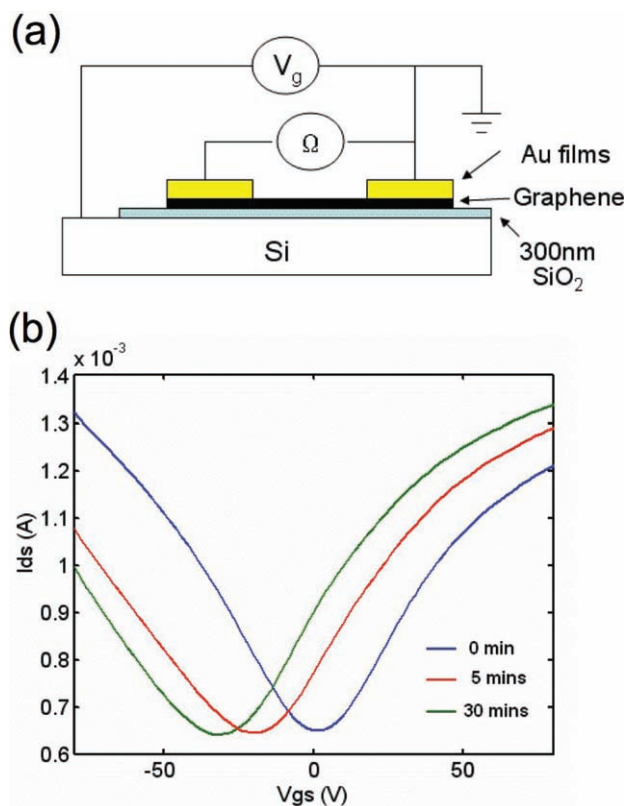
Figure 9. (a) Schematic of a graphene FET gas sensor device; (b) Evolution of I_{ds}-V_{gs} curves with the exposure to NH_3 of the graphene FET for different durations.

was estimated.[137] A surface transfer doping, by surface modification of epitaxial graphene grown on 6H-SiC(0001) with appropriate molecular acceptors, has been proposed to achieve controllable p-doping in graphene.[138]

3.2. Sensors

Due to its conductance changing as a function of extent of surface adsorption, large specific surface area, and low Johnson noise,[1,49,50] recent experimental[52,139–143] and theoretical[144–146] research has demonstrated that monolayer graphene is a promising candidate to detect a variety of molecules, such as gases[52,139–141] to biomolecules.[142,143] Charge transfer between the adsorbed molecules and graphene is proposed to be responsible for the chemical response. As molecules adsorb to the surface of graphene, the location of adsorption experiences a charge transfer with graphene as a donor or acceptor, thus changing the Fermi level, carrier density, and electrical resistance of graphene. **Figure 9a** shows a typical schematic of a graphene FET device for sensing gas molecules. During the exposure of the device to gas (e.g., NH_3), the time evolution of source-drain current (I_{ds}) versus gate voltage (V_{gs}) was recorded (Figure 9b).[147] Initially, the Dirac point (V_D) is close to the back gate bias of 0 V; after 5 minutes of exposure, the Dirac point appears at −20 V and slowly shifts to its final position at about −30 V. These results suggest that NH_3 molecules adsorb

on the graphene surface and n-dope the graphene in the FET device. Based on the charge transfer rate and the Dirac point shift, the concentration of the molecules on the graphene surface was estimated as 8×10^{13} cm^{-2} after 30 minutes of exposure. Recent studies stated that NH_3 and CO molecules will act as donors while H_2O and NO_2 will act as acceptors on the graphene surface.[52,146] Moreover, reduced graphene oxide has been shown to be a good sensor, achieving sensitivities at parts-per-billion levels for detection of chemical warfare agents and explosives.[140,141] CMG has been used in biodevices as a sensor at both the biocellular and the biomolecular scale. It can act as an interface to recognize single bacteria, a label-free, reversible DNA detector, and a polarity-specific molecular transistor for protein/DNA adsorption.[142,143]

### 3.3. Transparent Conductive Films

With high electrical conductivity, high carrier mobility, and moderately high optical transmittance in the visible range of the spectrum, graphene materials show promise for transparent conductive films (TCFs). The scalability of production and convenient processing of GO has led to its emergence as an important precursor for the fabrication of TCFs. Data on graphene TCFs are listed in **Table 1**. Films containing graphene oxide platelets have been deposited via spin-coating,[19,148] dip-coating,[149] vacuum filtration,[150] and Langmuir-Blodgett (LB) assembly,[151] followed by chemical reduction and/or thermal annealing. Researchers have also developed various methods to obtain graphene or reduced graphene oxide suspensions for the preparation of TCFs.[152] For example, spray-coated TCFs from aqueous dispersions of reduced graphene oxide nanoplatelets were obtained by changing the pH to about 10 prior to reduction with hydrazine.[153] LB-assembled films consisting of overlapped and stacked CMG platelets yielded a sheet resistance of 8 kΩ□$^{-1}$ at a transparency of 83% (at a wavelength of 1000 nm).[154] Liquid-liquid assembly, occurring at the H_2O-chloroform interface, has been used to prepare films containing highly hydrophobic films consisting of multilayer graphene platelets, from which a sheet resistance of 100 Ω□$^{-1}$ was obtained with a optical transmittance of 70% at 500 nm.[155] Disordered films of randomly stacked few-layer graphene platelets, made by directly sonicating graphite in organic solvents followed by vacuum filtration,[156] have shown a sheet resistance of ~3 kΩ□$^{-1}$ at a transmittance of ~75% (at 550 nm).[157] Recently, the chemical reduction of graphene oxide platelets in a liquid dispersion and their spin-assisted assembly was achieved in one step in the fabrication of graphene based TCFs, from which a sheet resistance of 11.3 kΩ□$^{-1}$ corresponding to a transmittance of 87% at 550 nm was obtained.[158] Graphene TCFs have been used as electrodes for dye-sensitized solar cells,[149] liquid crystal devices,[159] and organic light-emitting diodes.[160]

The sheet resistance reported for CMG TCFs varies over a wide range due to the variety of surface functionalities and defects introduced as a byproduct of the production methods. On the other hand, CVD on metals offers the possibility of growing large area graphene films of reasonably high quality.[17,161,162] Table 1 shows that CVD of graphene films (on

Table 1. Sheet resistances and optical transmittance of typical graphene based thin films.

Graphene film	Resistance/Conductance	Transmittance (wavelength)	Ref
Spin coating of reduced graphene oxide –SiO_2 composite	0.45 Scm^{-1} (28nm thick)	95% (550 nm)	[19]
Spin coating of reduced graphene oxide	10^2–10^3 $\Omega\square^{-1}$	80% (550 nm)	[148]
Dip-coating of graphene oxide followed by reduction	550 Scm^{-1} (10nm thick)	70.7% (1000 nm)	[149]
Vacuum filtration of graphene oxide suspension, followed by reduction	4.3×10^4 $\Omega\square^{-1}$	73% (550 nm)	[150]
LB assembly of graphene oxide followed by reduction	1.9×10^7 $\Omega\square^{-1}$	95.4% (650 nm)	[151]
Spray coating of chemically modified graphene oxide suspension at pH 10	2×10^7 $\Omega\square^{-1}$	96% (600–1000 nm)	[153]
LB assembly of chemically modified graphene	8×10^3 $\Omega\square^{-1}$	83% (1000 nm)	[154]
Liquid-liquid assembly of graphene platelets	100 $\Omega\square^{-1}$	70% (500 nm)	[155]
Spin assisted self-assembly of reduced graphene oxide	1.1×10^4 $\Omega\square^{-1}$	87% (550 nm)	[158]
Vacuum filtration of graphene platelets made by sonication of graphite in n-methyl-2-pyrrolidone (NMP)	3×10^3 $\Omega\square^{-1}$	75% (550 nm)	[157]
Spray deposition of graphene platelets made by sonicating graphite in dimethylformammide (DMF)	5×10^3 $\Omega\square^{-1}$	90%	[159]
CVD grown graphene on Ni followed by transfer	280 $\Omega\square^{-1}$	76% (550 nm)	[161]
CVD grown graphene on Cu followed by transfer	350 $\Omega\square^{-1}$	90% (550 nm)	[7]
CVD grown graphene on Ni followed by transfer	200 $\Omega\square^{-1}$	85% (550 nm)	[163]
CVD grown graphene on Ni followed by transfer	770 $\Omega\square^{-1}$	90% (500–1000 nm)	[162]

metal substrates with subsequent transfer to insulating and transparent substrates) has yielded lower sheet resistances for similar transparency values. Stretchable transparent electrodes were produced by transferring graphene grown on Ni onto polydimethylsiloxane (PDMS) substrates.[161] With a minimum sheet resistance of ~280 $\Omega\square^{-1}$ at a transparency of ~76% (at 550 nm), graphene TCFs were stated to withstand a tensile strain of 6.5% with little resistance increase and the original resistance could be restored after a tensile strain of 18.7%. To minimize the density of cracks caused during the transfer process, an improved transfer process for the preparation of large area (up to 4.5×4.5 cm^2) graphene TCFs on cover glass, quartz, or poly(methyl methacrylate) (PMMA) substrates was reported.[7] As shown in **Figure 10a**, a sheet resistance of 350 $\Omega\square^{-1}$ was obtained from four layers of graphene sequentially transferred onto cover glass while maintaining a relatively high transmittance of 90% (at 550 nm). Moreover, the monolayer graphene transferred onto PMMA followed by transfer onto a polyethylene terephthalate (PET) substrate has shown a resistance independent on the tensile bending of up to 5% strain, even after 100 bending cycles (Figure 10b). In another work, the dependence of the sheet resistance on the transmittance of few-layer graphene films grown on Ni or Cu followed by a transfer onto cover glass was studied.[6] It was found that the relationship between resistance
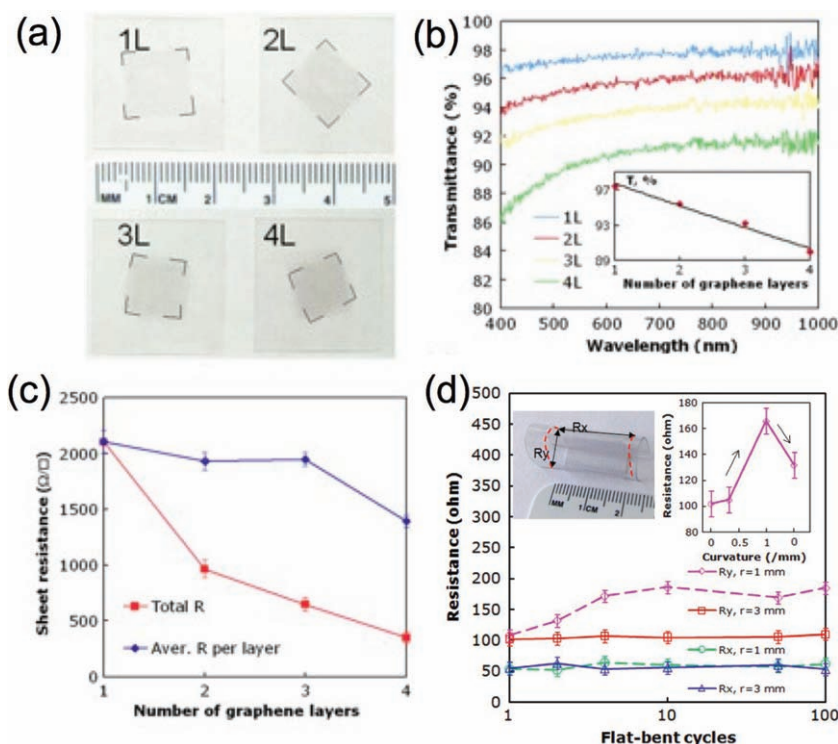
Figure 10. (a) Photographs of 1 cm^2 films of stacked graphene (one to four layers) on cover glass slips; (b) Transmittance of n-layer graphene films shown in (a). The inset is the relationship between the transmittance, T (%), at $\lambda = 550$ nm as a function of the number of stacked graphene layers, n; (c) Sheet resistance of n-layer graphene films as a function of the number of stacked graphene layers, n; (d) Resistance of graphene/PMMA films with different bending radii and flat-fold cycles. The top left inset shows the photo of bent graphene/PMMA/PET. The red dashed lines mark the edges of graphene/PMMA film. The top right inset shows the changes of R_y as a function of bending radius. Reproduced with permission from.[7] Copyright: 2009 American Chemistry Society.
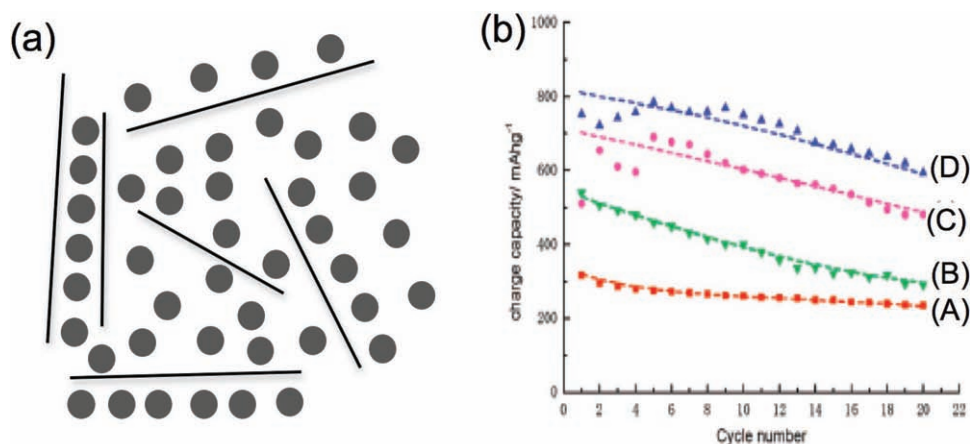
Figure 11. (a) A model of lithium adsorption on the two sides of an isolated graphene sheet; (b) Lithium insertion/extraction properties of graphene nanosheets (GNS): Charge/discharge cycle performance of (A) graphite, (B) GNS (C) GNS + CNT (D) GNS + C_{60}. Reproduced with permission from[165] (a) and[166] (b). Copyright: 1996 Elsevier Science Ltd and 2008 American Chemistry Society (b).

and transmittance generally followed the trend predicted by the Beer-Lambert law; a sheet resistance of 200 $\Omega\square^{-1}$ was obtained for a transmittance of 85% (at 550 nm). Considering the argument that the intrinsic sheet resistance of graphene is about 30 $\Omega\square^{-1}$,[163] there is still potential for improving the quality of graphene for use in TCF devices.

3.4. Clean Energy Devices

Graphene is a promising electrode material due to its high theoretical surface area of 2630 m^2g^{-1} and ability to facilitate electron or hole transfer along its two-dimensional surface. There have been several reports on graphene-based electrodes for both rechargeable lithium ion batteries (RLBs) and electrochemical double layer capacitors (EDLCs). Graphite, the most commonly used anode material in RLBs, has a maximum 'lithium insertion' capacity of 372 $mAhg^{-1}$, corresponding to the formation of a graphite intercalation compound consisting of one lithium ion to every six carbon atoms (LiC_6).[164] However, monolayer graphene in disordered carbon has been proposed to bind lithium ions on both its surfaces to achieve a Li_2C_6 stoichiometry (**Figure 11a**).[165] A specific capacity of 540 $mAhg^{-1}$ for anodes composed of reduced graphene oxide platelets was reported, and incorporation of CNT and C_{60} in these types of anodes was reported to increase the capacity to 730 and 784 $mAhg^{-1}$, respectively (Figure 11b).[166] The increased storage capacity was attributed to the increase in interlayer distance between the graphene platelets caused by either the CNTs or C_{60} molecules. Graphene nanosheets prepared by electron beam irradiation of graphene oxide suspensions exhibited a higher reversible capacity of 784 $mAhg^{-1}$ after 15 cycles; the enhanced capacity was attributed to additional storage sites such as edges and defects.[167] Flexible 'graphene paper' electrodes displayed poor electrochemical performance compared to powder composed of reduced graphene oxide platelets, in spite of the good conductivity and mechanical stability of such paper samples.[168] However, when silicon nanoparticles were mixed with reduced graphene oxide platelets in a paper-like material, a storage capacity >2200 $mAhg^{-1}$ after 50 cycles and >1500 $mAhg^{-1}$ after 200 cycles was obtained recently.[169] It was stated that the uniform dispersion of silicon particles in the composites and the reconstitution of graphene platelets to from a continuous, highly conducting 3D network are important for the high storage capacities.

Encapsulating metal or metal oxide particles with graphene or graphene-based carbonaceous materials has been evidently effective in overcoming the problem of volume expansion in pure metal/metal oxide electrodes.[170,171] Moreover, the structural flexibility and superior conductivity of reduced graphene oxide were reported to enhance the electrode performance of metal-graphene hybrids. A graphene-SnO_2 composite anode showed increased reversible capacity (570 mAh/g after 15 cycles) and superior cyclic performances compared to bare SnO_2 particles (60 $mAhg^{-1}$).[172,173] Other nanostructured metal oxide-graphene hybrids are being reported to perform better than their host metal oxide nanoparticle electrodes.[174–176] Recently, a Sn-graphene nanocomposite has been shown to reach a reversible capacity of 810 $mAhg^{-1}$ along with an average coulombic efficiency of 96.5% for 100 cycles.[177] In this report, the tin nanoparticles were held as spacers between the graphene sheets forming a 3D structure. More effort towards addressing issues such as irreversible capacity loss is evidently called for.

EDLCs are non-faradaic ultracapacitors which store charge in electric double layers formed at the interface between a high surface area electrode and an electrolyte.[178] Activated carbons having high specific surface area (typically supplemented with a more conductive filler such as carbon black) are extensively used as electrode materials in EDLCs.[179] CMG are a new type of carbon for study and potential use as an electrode material for ultracapacitors.[180,181] As shown in **Figure 12**, an ultracapacitor based on CMG electrodes exhibited specific capacitances of 135 Fg^{-1} and 99 Fg^{-1} with aqueous and organic electrolytes, respectively. With other techniques of exfoliation and reduction of GO, e.g., using microwave irradiation[182] or directly heating a suspension of graphene oxide platelets in propylene carbonate (PC),[183] capacitance values as high as 190 Fg^{-1}
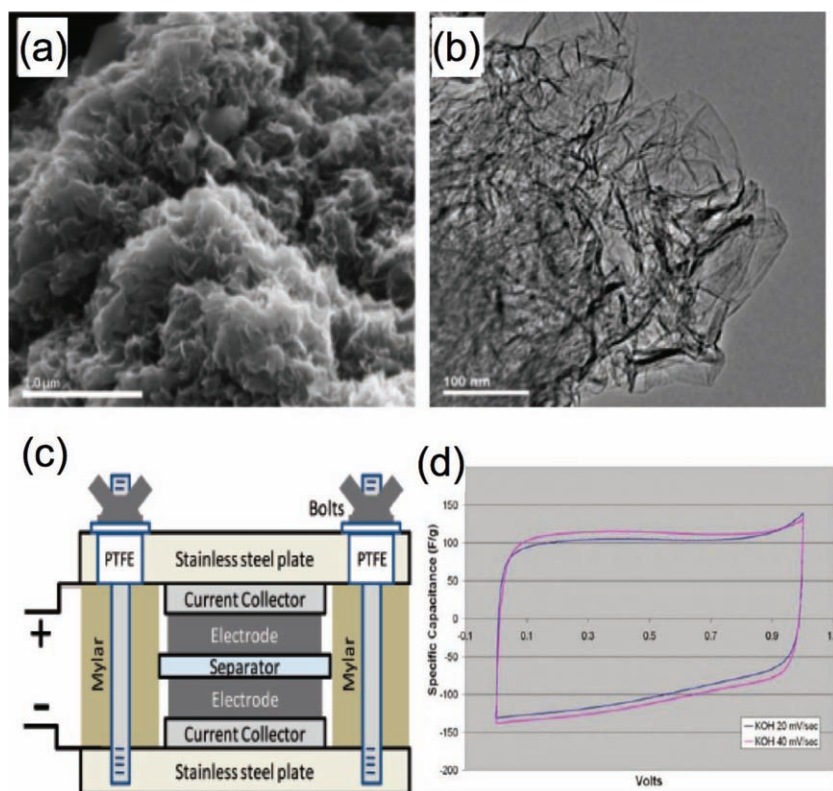
Figure 12. (a) SEM image of the surface of 'particles' composed of agglomerated CMG platelets; (b) TEM image showing individual CMG platelets extending from a particle composed of agglomerated CMG platelets; (c) schematic of the ultracapacitor test cell assembly; (d) CV plots obtained from cyclic voltammogram measurements of electrodes consisting of the CMG material, with KOH electrolyte. Reproduced with permission from.[180] Copyright: 2008 American Chemistry Society.

surface area.[186] Several groups have reported graphene-based ultracapacitors using metal oxide/graphene,[187–189] CNTs,[190] and polymer/graphene composites for electrodes/graphene.[191–194] **Table 2** shows reported results for ultracapacitors with graphene-based materials as the electrodes.

Graphene materials have also been used in studies of hydrogen storage, fuel cells, and solar cells. For example, CMG made by reducing graphene oxide with hydrazine and with a Brunauer-Emmett-Teller (BET) specific surface area of 640 m^2g^{-1} (when dried down), has shown a hydrogen adsorption capacity of 0.68 wt% at 77K and 1 bar.[195] This value was expected to be increased by further increasing the surface area of graphene materials. Graphene has been identified as a catalyst support for oxygen reduction and methanol oxidation in a fuel cell configuration.[196–200] Conductive graphene scaffolds for platinum nanoparticles facilitated efficient collection and transfer of electrons to the electrode surface. Graphene based materials have been used as both the window electrode and counter electrode in dye sensitized solar cells.[201,202] Graphene-doped conducting polymers such as Poly(3,4-ethylenedioxythiophene)poly(styrenesulfonate) (PEDOT:PSS) and poly(3-hexylthiophene) (P3HT) have shown better power consumption efficiency (4.5%) than cells with PEDOT:PSS as a counter electrode (2.3%).[203]

in aqueous and 120 Fg^{-1} in organic electrolytes have been achieved. Graphene materials made by thermally expanding GO at high temperatures,[184] or alternatively at relatively low temperatures (e.g., 200 °C) under vacuum (<1 Pa),[185] have been used as ultracapacitor electrodes. There are also ongoing efforts to make graphene composites with spacers in order to prevent agglomeration of graphene platelets and increase the accessible

3.5. Graphene-Polymer Nanocomposites

Graphene–based fillers have been used in polymer nanocomposites and hold potential for a variety of possible applications.[204] GO and other graphite derivatives such as graphite intercalation compounds (GICs) can be used as precursors to bulk scale production of an assortment of exfoliated

Table 2. Specific surface areas and capacitance values of graphene based ultracapacitors.

| Graphene material	Specific surface area in m^2g^{-1}	Specific capacitance in Fg^{-1} (electrolyte)	Ref
Chemically reduced graphene oxide	705	135 (KOH) 99 (Organic)	[180]
Chemically reduced graphene oxide	320	205 (KOH)	[181]
Microwave expanded GO	463	191 (KOH)	[182]
Thermally reduced graphene oxide in PC	—	122 (Organic)	[183]
Thermally expanded GO at 1050 °C	925	117(H_2SO_4) 75 (Ionic liquid)	[184]
Thermally expanded GO at 200 °C in vacuum	368	264 (KOH) 122 (Organic)	[185]
Reduced graphene oxide-SnO_2 composite	—	43 (H_2SO_4)	[188]
Graphene oxide-MnO_2 composite	—	216 (Na_2SO_4)	[189]
Polymer modified graphene/carbon nanotube hybrid film	—	120 (H_2SO_4)	[190]
1% Graphene oxide doped polyaniline	—	531 (H_2SO_4)	[193]
Chemically modified graphene /polyaniline nanofiber composite film	12.7	210 (H_2SO_4)	[194]

CMGs or 'graphite nanoplatelets' for use as a filler.[21] Polymer matrix composites with graphene-based filler include polystyrene (PS),[18,205–207] PMMA,[208] polyvinyl alcohol (PVA),[209–211] polypropylene (PP),[212,213] epoxy,[214–217] polyester,[218] silicone foam,[219] polyurethane,[220,221] poly(vinyldiene fluoride),[222] and polycarbonate.[223] To achieve large property enhancements in their nanocomposites, layered materials such as GO must be exfoliated and well dispersed in the polymer matrix.[224] Among other methods, rapid heating,[21,225] as well as ultrasonication of GO have been used extensively to produce highly-exfoliated platelets for nanocomposites; notably, themally-expanded GO('TEGO') is reduced and can be use to make electrically conductive composites,[21] whereas mechanically-exfoliated GO retains its insulating chemical structure and must be reduced in a separate step.[30] These fillers can be dispersed into polymers using techniques such as solution mixing, melt blending, or *in situ* polymerization; of these methods, *in situ* polymerization might offer superior dispersion of this filler.[212]

Polymer nanocomposites with GO-derived graphene materials as filler have shown dramatic improvements in properties such as elastic modulus, tensile strength, electrical conductivity, and thermal stability. Moreover, these improvements are often observed at low loadings of filler evidently due to the large interfacial area and high aspect ratio of these materials, requiring small amounts of filler to achieve percolation.[208,226] At 0.7 wt% loading, a solution-mixed PVA-graphene oxide nanocomposite showed a 76% increase in tensile strength and a 62% increase in Young's modulus; the results were attributed to effective load transfer to the graphene oxide filler via interfacial hydrogen bonding.[209] Chemical reduction of graphene oxide in the presence of PVA generated conductive composites with a percolation threshold below 1 wt% and produced large shifts in glass transition temperature, T_g.[210] Large increases in Young's modulus and a 30 °C shift in T_g at only 0.05 wt% loading of a TEGO-PMMA composite were attributed to the onset of rheological percolation and to the crumpled morphology of the highly-exfoliated platelets.[208] Nanocomposites of platelets derived from TEGO have shown higher stiffness across all loadings and equal or lower electrical percolation thresholds than carbon black and nanotube-filled nanocomposites.[226] Low loadings of exfoliated GO platelets in epoxy reduced the coefficient of thermal expansion (up to 32% at 5 wt%)[216] and increased the critical buckling strength (by 52% at 0.1 wt%) versus the neat polymer.[215]

Covalent functionalization of exfoliated GO and acid-treated graphite platelets has been used in an effort to compatibilize the filler with polymer hosts for improved dispersion. For instance, isocyanate-functionalized graphene oxide was mixed with PS in a solution, and subsequent reduction yielded conductive nanocomposites with an onset of electrical percolation at 0.1 vol%, consistent with some of the lowest thresholds reported, e.g., for CNT nanocomposites (**Figure 13**).[18] Acid-treated and exfoliated graphite was functionalized with PVA via ester linkages, yielding composites with well-dispersed graphene particles that showed a 20°C shift in T_g,[227] while silane-functionalized expanded graphite (EG) resulted in a 35% improvement over unmodified EG-epoxy nanocomposites.[214] Covalent grafting of PS microspheres to reduced graphene oxide has been reported using emulsion polymerization.[206] Recently, growth of polymer chains from graphene oxide has been demonstrated using atom transfer radical polymerization (ATRP), following functionalization of the surface with initiator. Grafted polymers dramatically improved the solubility of graphene oxide in organic solvents,[207,228] while nanocomposites of PS-grafted graphene oxide in a PS matrix demonstrated substantial mechanical property enhancements (57% increase in modulus and 70% increase in strength at 0.9 wt%).[205]

Novel synthesis and processing methods have produced graphene/'graphite nanoplatelet' nanocomposites with large property improvements, unique structures, and some of the lowest percolation thresholds reported to date. For instance, layer-by-layer assembly created conductive PVA-CMG nanocomposites[211] while solid state shear pulverization was used to directly exfoliate graphite in PP, doubling the modulus versus the neat polymer.[213] A simple method of coating polymer powder with graphite nanoplatelets prior to melt blending resulted in a dramatic reduction in the percolation threshold of a PP nanocomposite from 7 wt% to 0.1 wt%,[212] while a 'reduction-extractive' dispersion technique yielded conductive
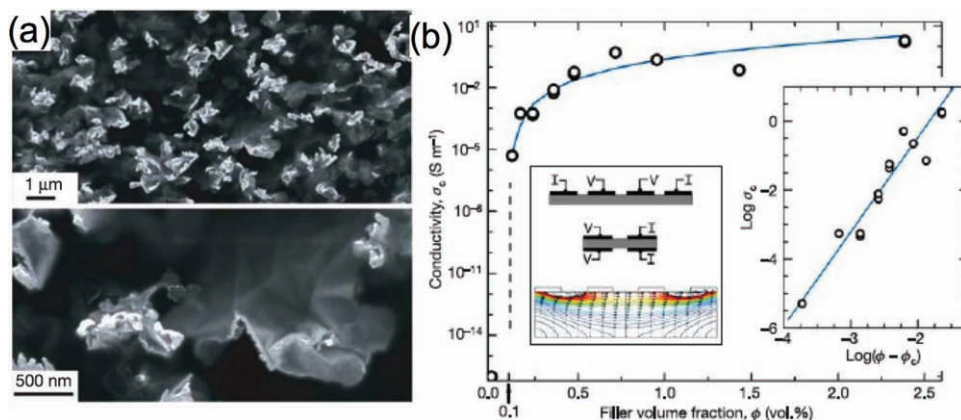
Figure 13. (a) Low (top) and high (bottom) magnification SEM images obtained from a fracture surface of composite samples of 0.48 vol.% 'graphene' (phenyl isocyanate treated and 1,1 dimethylhydrazine-reduced graphene oxide) in polystyrene; (b) Electrical conductivity of the polystyrene–'graphene' composites as a function of filler volume fraction. Reproduced with permission from.[18] Copyright: 2006 Nature Publishing Group.

**ADVANCED
MATERIALS**

www.advmat.de

*Materials
Views*

www.MaterialsViews.com

REVIEW

reduced graphene oxide-vinyl acetate/vinyl chloride copolymer nanocomposites with a percolation threshold of 0.15 vol%.[229] Reduction of GO with polysulfide ions led to sulfur nanoparticle-decorated graphene oxide, which were then melt blended with poly(arylene sulfide), yielding highly exfoliated platelets in the matrix.[230] Aqueous solutions of PVA mixed with polystyrene sulfonate-stabilized graphene oxide were frozen and freeze-dried to produce nanocomposite monoliths with a 3D, porous scaffold-like structure that might find applications in electronics and as catalyst supports.[231]

4. Synthesis

4.1. Graphene

There are now four primary ways to produce 'pristine' graphene.

Epitaxial graphene. This method involves CVD growth on epitaxially matched metal surfaces. John May explained in an article published in *Surface Science* in 1969 how published but (at that time) unassigned low-energy electron diffraction (LEED) patterns could be rationalized in terms of a "monolayer of graphite."[232] Blakely and his group undertook detailed scientific studies of the thermodynamics of growth of 'monolayer graphite' and of 'bilayer graphite' on Ni (111) crystals, publishing a series of insightful papers in the 1970s,[233–236] and a 'sub-discipline' of surface science developed on the topic 'monolayer graphite' or 'MG', that continues to this day (surface scientists now typically refer to the MG they grow as graphene). A more recent thrust in terms of growth of epitaxial graphene, is its large-area growth on SiC wafer surfaces by high temperature (>1300 °C) evaporation of Si in either ultrahigh vacuum (UHV)[16,237,238] or atmospheric pressure[239] as a method to prepare wafer-size graphene with carrier mobility values of about 2000 cm^2 V^{-1} s^{-1}.[239] Atomically resolved STM has been used to study the bottom-up formation of graphene on the single crystal SiC surface.[240] Large area monolayer graphene has been achieved on Cu films,[7,17,241] and this method can be in principle extended to 'endless length, very large width' production simply by exposing appropriate metal foils to C to achieve surface deposition of either monolayer or multilayer. (It is of interest that epitaxial growth has not yet been proven (or disproven) for growth on Cu, and so this might eventually be classified as another method for growth of graphene—such as non-epi growth.) This category might end up including the possibility of growth from (or on) molten metals and amorphous metal substrates. Direct growth of graphene on metal oxide surfaces is an exciting challenge that could benefit, e.g., nanoelectronics. To our knowledge, this has not yet been achieved.

Micromechanical Exfoliation. Ruoff and coauthors laid the foundation for micromechanical exfoliation as well as outlined the potential importance for graphene for a wide variety of fundamental studies and applications, in several papers published in 1999.[13,14] This work inspired physicists to try methods such as rubbing lithographically patterned pillars with "tipless" AFM cantilevers,[242] and using of Scotch tape to achieve very thin platelets of graphite. Micromechanical exfoliation can be used to generate 'high quality' graphene that is electrically isolated for fundamental studies of transport physics and other properties, but does not yet appear to be scalable to large area. It typically produces graphene 'particles' with lateral dimensions on the order of tens to hundreds of micrometers. However, there have been attempts, from patterned graphite using the pillar approach invented by Ruoff, to achieve patterned graphene by micromechanical exfoliation.[13,14]

Exfoliation of graphite in solvents. A third method inspired by, e.g., obtaining dispersions of GO to yield individual layers of graphene oxide (i.e., colloidal dispersions) is to make dispersions of graphite in various solvents; this is typically done by exposure of graphite powders in organic solvents such as DMF or NMP to high intensity ultrasound,[156] and while significant progress has been made, the yield is relatively low. (One notes the paper in 1962 by Boehm et al., that presented TEM results that pinpointed the presence of individual layers of reduced graphene oxide, by densitometry analysis of TEM images.[243])

'Other methods'. Substrate-free gas-phase synthesis of graphene platelets in a microwave plasma reactor[244] and arc-discharge synthesis of multi-layered graphene[245] have also recently been reported. It seems likely that reports of gas phase synthesis of 'graphene powders' will increase in the future, and the authors suggest it as an important area of research. Large scale production of 'powdered' graphene of high C purity by CVD approaches (including thermal CVD, etc.) could provide material in sufficient quantity for a host of likely applications, as well as for fundamental science.

As mentioned, graphene can be grown on metal surfaces by surface segregation of carbon or by decomposition of hydrocarbons. However, this technique is only practical for graphene production if the as-grown graphene can be transferred from the metal substrates to other substrates, which looks straightforward but only was realized for multilayer and non-uniform films recently with Ni,[161,162,246] and for uniform monolayer graphene, with Cu.[17] In contrast to the use of high-cost single crystal metals and UHV systems in previous work by the surface science community, few-layer graphene films were grown on polycrystalline Ni foils by CVD of methane under atmospheric pressure by controlling the cooling rate of the metal substrates so as to suppress carbon precipitation during cool-down.[246] Few-layer graphene films were also grown on thin Ni films from which the amount of precipitated C was also suppressed.[161,162] However, because the solubility of C in Ni is relatively high, it has to date been difficult to suppress C precipitation completely so that the produced graphene films vary from monolayer to tens of layers. Instead, large-area films with >95% as monolayer graphene were grown on Cu foils by CVD of methane by taking advantage of the very low solubility of C in Cu (**Figure 14**).[17] By using ^{13}C labeling, it was shown that graphene growth on Cu is a surface-mediated process and the process is self-limiting; that is, once the Cu surface was fully covered with graphene, the growth process terminated; also it was possible to achieve 100% monolayer coverage.[241] Graphene grown on metal substrates also shows high quality with extracted carrier mobilities typically in the range 2000 to 4000 cm^2 V^{-1} s^{-1}. These values are lower than values for those from particular flakes (chosen by various researchers as values to report) made by micromechanical exfoliation. Improvement of quality of the CVD grown graphene in terms of synthesis, and also in terms of transfer to

Materials Views
www.MaterialsViews.com

ADVANCED
MATERIALS
www.advmat.de

REVIEW
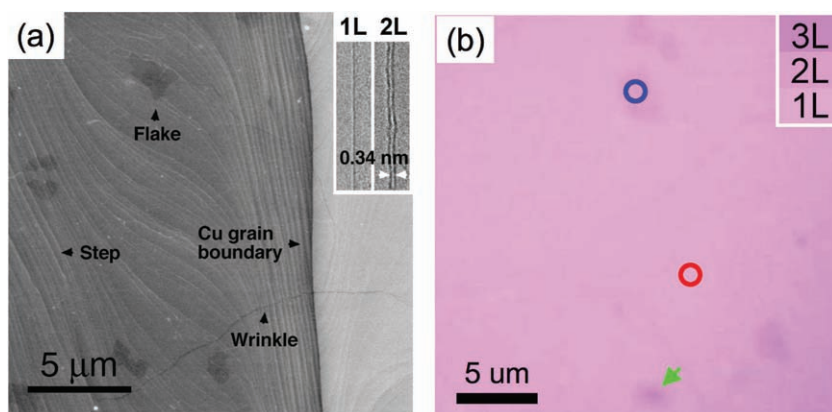
Figure 14. (a) SEM image showing a Cu grain boundary and steps in the Cu substrate surface, 2- and 3-layer thick graphene flakes, and wrinkles in the graphene film. Inset shows TEM images of edges of folded graphene; (b) Optical microscope image of graphene film transferred onto a SiO_2 (285 nm)-on-Si substrate showing wrinkles, and 2- and 3-layer regions. Reproduced with permission from.[17] Copyright: 2009 American Association for the Advancement of Science.

arbitrary substrates, is desirable. But another question perhaps never asked in the literature, and thus posed here, is: What number of flakes of monolayer graphene made by micromechanical exfoliation have been interrogated to obtain parameters such as gate voltage of the Dirac point, impurity concentration at the Dirac point, and mobility? Private remarks by researchers in the field suggest that only the "very best" flakes are studied, and that there may be a relatively large fraction that are "not reported", and this might come as no surprise. One goal of physics is to find high quality specimens and "milk them for all they are worth", such as for transport measurements.

4.2. Graphite Oxide

Comprehensive reviews on the preparation of dispersions of graphene oxide platelets and reduced graphene oxide platelets, made from GO, have recently appeared.[30,152] In general, GO is synthesized by either the Brodie,[25] Staudenmaier,[247] or Hummers method,[248] or some variation of these methods. All three methods involve oxidation of graphite to various levels. Brodie and Staudenmaier used a combination of potassium chlorate ($KClO_3$) with nitric acid (HNO_3) to oxidize graphite, and the Hummers method involves treatment of graphite with potassium permanganate ($KMnO_4$) and sulfuric acid (H_2SO_4). Graphite salts made by intercalating graphite with strong acids such as H_2SO_4, HNO_3 or $HClO_4$ have also been used as precursors for the subsequent oxidation to GO.[249] **Figure 15** shows a proposed structure of graphene oxide that is supported by solid-state nuclear magnetic resonance (SSNMR) experiments on ^{13}C-labeled GO;[250] and see references therein for discussion of prior studies and various models proposed for the structure of graphene oxide.

The polar oxygen functional groups of GO render it hydrophilic; GO can be exfoliated in many solvents, and disperses particularly well in water.[251] Dispersions of graphene oxide platelets can be obtained by stirring and more typically by sonication of GO in solvents; chemical reduction of the colloidal dispersions obtained has been performed with several reducing agents, such as them hydrazine,[252] hydroquinone,[253] sodium borohydride ($NaBH_4$),[254,255] and ascorbic acid.[256] Reduction via thermal treatment[225,257] has been reported to be an efficient and low cost method, producing 'TEGO' material with a BET surface area of 600–900 m^2/g. Electrochemical reduction has been presented as an effective way to remove oxygen functional groups from GO.[258] Chemical reduction using $NaBH_4$ followed by a H_2SO_4 treatment prior to thermal annealing yielded CMG platelets with high C purity.[259] The detailed chemistry of oxidation and also reduction, and the chemical tuning of graphene platelets is an active area of research that should continue to rapidly grow.[260]

5. Conclusions and Perspective

In this article, the preparation, properties, and applications of graphene-based materials have been reviewed.

Preparation of high quality graphene materials in a cost-effective manner and on the desired scale is essential for many applications. CVD growth on metal foils has exceptional potential for, ultimately, the production of endless lengths of graphene/n-layer graphene of desired widths ('graphene foil') that could then be picked up by roll-to-roll processing. Further improvement of the quality along with development of a clean transfer process for such foils will help to realize many applications including graphene-based electronic devices, for thermal management, for transparent conductive electrodes, and others. Fine control of the number of graphene layers for n-layer graphene (with the exception of monolayer graphene) is an important challenge
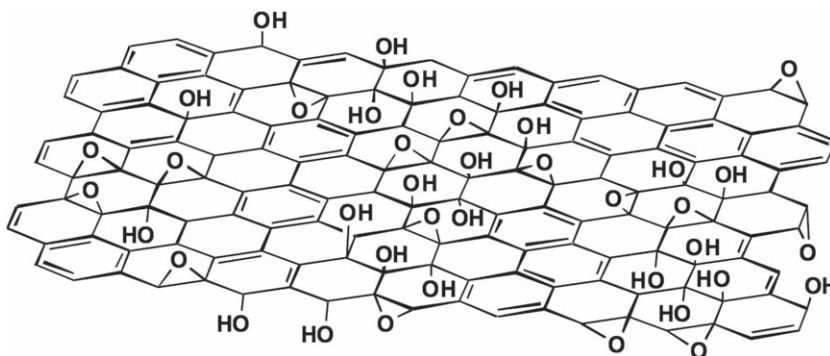
Figure 15. A proposed schematic (Lerf-Klinowski model) of graphene oxide structure. Reproduced with permission from [H. He, J. Klinowski, M. Forster and A. Lerf, Chem. Phys. Lett., 1998, 287, 53–56]. Copyright: 1998 Elsevier Science Ltd.

for the materials community, such as for fundamental studies of bi-layer and tri-layer graphene, and to understand the performance (as one example among many targeted applications) as TCF's. The preparation of graphene materials via 'chemical' processing routes (e.g., oxidation of graphite followed by reduction of the graphene oxide platelets obtained by exfoliation) may be able to produce fairly large amounts of 'graphene' cost effectively; however, the chemical details (e.g., oxidation/reduction mechanisms and detailed chemical structures) need to be more fully understood. Future efforts for graphene and n-layer graphene such as achieving desired surface functionalization, and, e.g., the 'cutting' or preparation into desired shapes, could generate novel structures having many applications.

Acknowledgements

[1] A. K. Geim, K. S. Novoselov, *Nat. Mater.* **2007**, *6*, 183.

[2] K. I. Bolotin, K. J. Sikes, Z. Jiang, M. Klima, G. Fudenberg, J. Hone, P. Kim, H. L. Stormer, *Solid State Commun.* **2008**, *146*, 351.

[3] S. V. Morozov, K. S. Novoselov, M. I. Katsnelson, F. Schedin, D. C. Elias, J. A. Jaszczak, A. K. Geim, *Phys. Rev. Lett.* **2008**, *100*, 016602.

[4] C. Lee, X. D. Wei, J. W. Kysar, J. Hone, *Science* **2008**, *321*, 385.

[5] A. A. Balandin, S. Ghosh, W. Z. Bao, I. Calizo, D. Teweldebrhan, F. Miao, C. N. Lau, *Nano Lett.* **2008**, *8*, 902.

[6] W. Cai, Y. Zhu, X. Li, R. D. Piner, R. S. Ruoff, *Appl. Phys. Lett.* **2009**, *95*, 123115.

[7] X. Li, Y. Zhu, W. Cai, M. Borysiak, B. Han, D. Chen, R. D. Piner, L. Colombo, R. S. Ruoff, *Nano Lett.* **2009**, *9*, 4359.

[8] H. P. Boehm, A. Clauss, G. O. Fischer, U. Hofmann, *Z. Anorg. Allg. Chem.* **1962**, *316*, 119.

[9] H. P. Boehm, R. Setton, E. Stumpp, *Pure Appl. Chem.* **1994**, *66*, 1893.

[10] H. P. Boehm, R. Setton, E. Stumpp, *Carbon* **1986**, *24*, 241.

[11] J. Wintterlin, M. L. Bocquet, *Surf. Sci.* **2009**, *603*, 1841.

[12] A. J. Vanbommel, J. E. Crombeen, A. Vantooren, *Surf. Sci.* **1975**, *48*, 463.

[13] X. K. Lu, M. F. Yu, H. Huang, R. S. Ruoff, *Nanotechnology* **1999**, *10*, 269.

[14] X. K. Lu, H. Huang, N. Nemchuk, R. S. Ruoff, *Appl. Phys. Lett.* **1999**, *75*, 193.

[15] K. S. Novoselov, A. K. Geim, S. V. Morozov, D. Jiang, Y. Zhang, S. V. Dubonos, I. V. Grigorieva, A. A. Firsov, *Science* **2004**, *306*, 666.

[16] C. Berger, Z. M. Song, T. B. Li, X. B. Li, A. Y. Ogbazghi, R. Feng, Z. T. Dai, A. N. Marchenkov, E. H. Conrad, P. N. First, W. A. De Heer, *J. Phys. Chem. B* **2004**, *108*, 19912.

[17] X. S. Li, W. W. Cai, J. H. An, S. Kim, J. Nah, D. X. Yang, R. Piner, A. Velamakanni, I. Jung, E. Tutuc, S. K. Banerjee, L. Colombo, R. S. Ruoff, *Science* **2009**, *324*, 1312.

[18] S. Stankovich, D. A. Dikin, G. H. B. Dommett, K. M. Kohlhaas, E. J. Zimney, E. A. Stach, R. D. Piner, S. T. Nguyen, R. S. Ruoff, *Nature* **2006**, *442*, 282.

[19] S. Watcharotone, D. A. Dikin, S. Stankovich, R. Piner, I. Jung, G. H. B. Dommett, G. Evmenenko, S. E. Wu, S. F. Chen, C. P. Liu, S. T. Nguyen, R. S. Ruoff, *Nano Lett.* **2007**, *7*, 1888.

[20] D. A. Dikin, S. Stankovich, E. J. Zimney, R. D. Piner, G. H. B. Dommett, G. Evmenenko, S. T. Nguyen, R. S. Ruoff, *Nature* **2007**, *448*, 457.

[21] S. Park, R. S. Ruoff, *Nat. Nanotechnol.* **2009**, *4*, 217.

[22] M. Taghioskoui, *Mater. Today* **2009**, *12*, 34.

[23] D. W. Boukhvalov, M. I. Katsnelson, *J. Phys. Condens. Matter* **2009**, *21*.

[24] M. Segal, *Nat. Nano* **2009**, *4*, 612.

[25] B. C. Brodie, *Ann. Chim. Phys.* **1860**, *59*, 466.

[26] M. J. Allen, V. C. Tung, R. B. Kaner, *Chem. Rev.* **2009**, *110*, 132.

[27] C. N. R. Rao, A. K. Sood, K. S. Subrahmanyam, A. Govindaraj, *Angew. Chem. Int. Ed.* **2009**, *48*, 7752.

[28] C. Soldano, A. Mahmood, E. Dujardin, *Carbon* **2010**, *48*, 2127.

[29] C. N. R. Rao, A. K. Sood, R. Voggu, K. S. Subrahmanyam, *J. Physi. Chem. Lett.* **2010**, *1*, 572.

[30] D. R. Dreyer, S. Park, C. W. Bielawski, R. S. Ruoff, *Chem. Soc. Rev.* **2010**, *39*, 228.

[31] K. P. Loh, Q. Bao, P. K. Ang, J. Yang, *J. Mater. Chem.* **2010**, *20*, 2277.

[32] S. Unarunotai, Y. Murata, C. E. Chialvo, N. Mason, I. Petrov, R. G. Nuzzo, J. S. Moore, J. A. Rogers, *Adv. Mater.* **2010**, *22*, 1072.

[33] A. Fasolino, J. H. Los, M. I. Katsnelson, *Nat. Mater.* **2007**, *6*, 858.

[34] J. C. Meyer, A. K. Geim, M. I. Katsnelson, K. S. Novoselov, T. J. Booth, S. Roth, *Nature* **2007**, *446*, 60.

[35] E. Stolyarova, K. T. Rim, S. M. Ryu, J. Maultzsch, P. Kim, L. E. Brus, T. F. Heinz, M. S. Hybertsen, G. W. Flynn, *Proc. Nat. Acad. Sci. USA* **2007**, *104*, 9209.

[36] A. Deshpande, W. Bao, F. Miao, C. N. Lau, B. J. LeRoy, *Phys. Rev. B* **2009**, *79*, 205411.

[37] Y. B. Zhang, V. W. Brar, C. Girit, A. Zettl, M. F. Crommie, *Nat. Phys.* **2009**, *5*, 722.

[38] M. L. Teague, A. P. Lai, J. Velasco, C. R. Hughes, A. D. Beyer, M. W. Bockrath, C. N. Lau, N. C. Yeh, *Nano Lett.* **2009**, *9*, 2542.

[39] K. Xu, P. Cao, J. R. Heath, *Nano Lett.* **2009**, *9*, 4446.

[40] W. Bao, F. Miao, Z. Chen, H. Zhang, W. Jang, C. Dames, C. N. Lau, *Nat. Nanotechnol* **2009**, *4*, 562.

[41] A. Hashimoto, K. Suenaga, A. Gloter, K. Urita, S. Iijima, *Nature* **2004**, *430*, 870.

[42] J. C. Meyer, C. O. Girit, M. F. Crommie, A. Zettl, *Nature* **2008**, *454*, 319.

[43] Z. Lee, K. J. Jeon, A. Dato, R. Erni, T. J. Richardson, M. Frenklach, V. Radmilovic, *Nano Lett.* **2009**, *9*, 3365.

[44] J. C. Meyer, C. Kisielowski, R. Erni, M. D. Rossell, M. F. Crommie, A. Zettl, *Nano Lett.* **2008**, *8*, 3582.

[45] C. O. Girit, J. C. Meyer, R. Erni, M. D. Rossell, C. Kisielowski, L. Yang, C. H. Park, M. F. Crommie, M. L. Cohen, S. G. Louie, A. Zettl, *Science* **2009**, *323*, 1705.

[46] X. T. Jia, M. Hofmann, V. Meunier, B. G. Sumpter, J. Campos-Delgado, J. M. Romo-Herrera, H. B. Son, Y. P. Hsieh, A. Reina, J. Kong, M. Terrones, M. S. Dresselhaus, *Science* **2009**, *323*, 1701.

[47] P. R. Wallace, *Physical Review* **1947**, *71*, 622.

[48] A. H. C. Neto, F. Guinea, N. M. R. Peres, K. S. Novoselov, A. K. Geim, *Rev. Mod. Phys.* **2009**, *81*, 109.

[49] K. S. Novoselov, A. K. Geim, S. V. Morozov, D. Jiang, M. I. Katsnelson, I. V. Grigorieva, S. V. Dubonos, A. A. Firsov, *Nature* **2005**, *438*, 197.

[50] Y. B. Zhang, Y. W. Tan, H. L. Stormer, P. Kim, *Nature* **2005**, *438*, 201.

[51] T. Durkop, S. A. Getty, E. Cobas, M. S. Fuhrer, *Nano Lett.* **2004**, *4*, 35.

[52] F. Schedin, A. K. Geim, S. V. Morozov, E. W. Hill, P. Blake, M. I. Katsnelson, K. S. Novoselov, *Nat. Mater.* **2007**, *6*, 652.

[53] X. Du, I. Skachko, A. Barker, E. Y. Andrei, *Nat. Nanotechnol.* **2008**, *3*, 491.

[54] K. S. Novoselov, Z. Jiang, Y. Zhang, S. V. Morozov, H. L. Stormer, U. Zeitler, J. C. Maan, G. S. Boebinger, P. Kim, A. K. Geim, *Science* **2007**, *315*, 1379.

Materials
Views
www.MaterialsViews.com

ADVANCED
MATERIALS
www.advmat.de

REVIEW

[55] V. P. Gusynin, S. G. Sharapov, *Phys. Rev. Lett.* **2005**, *95*, 146801.

[56] N. M. R. Peres, F. Guinea, A. H. C. Neto, *Physical Review B* **2006**, *73*, 125411.

[57] D. L. Miller, K. D. Kubista, G. M. Rutter, M. Ruan, W. A. de Heer, P. N. First, J. A. Stroscio, *Science* **2009**, *324*, 924.

[58] V. M. Apalkov, T. Chakraborty, *Phys. Rev. Lett.* **2006**, *97*, 126801.

[59] C. Toke, J. K. Jain, *Phys. Rev. B* **2007**, *75*, 245440.

[60] X. Du, I. Skachko, F. Duerr, A. Luican, E. Y. Andrei, *Nature* **2009**, *462*, 192.

[61] K. I. Bolotin, F. Ghahari, M. D. Shulman, H. L. Stormer, P. Kim, *Nature* **2009**, *462*, 196.

[62] S. V. Morozov, K. S. Novoselov, M. I. Katsnelson, F. Schedin, L. A. Ponomarenko, D. Jiang, A. K. Geim, *Phys. Rev. Lett.* **2006**, *97*, 016801.

[63] M. I. Katsnelson, *Eur. Phys. J. B* **2006**, *51*, 157.

[64] N. Stander, B. Huard, D. Goldhaber-Gordon, *Phys. Rev. Lett.* **2009**, *102*, 026807.

[65] G. Van Lier, C. Van Alsenoy, V. Van Doren, P. Geerlings, *Chem. Phys. Lett.* **2000**, *326*, 181.

[66] C. D. Reddy, S. Rajendran, K. M. Liew, *Nanotechnology* **2006**, *17*, 864.

[67] K. N. Kudin, G. E. Scuseria, B. I. Yakobson, *Phys. Rev. B* **2001**, *64*, 235406.

[68] I. W. Frank, D. M. Tanenbaum, A. M. Van Der Zande, P. L. McEuen, *J. Vac. Sci. Technol. B* **2007**, *25*, 2558.

[69] M. Poot, H. S. J. Van Der Zant, *Appl. Phys. Lett.* **2008**, *92*.

[70] C. Gomez-Navarro, M. Burghard, K. Kern, *Nano Lett.* **2008**, *8*, 2045.

[71] S. Park, K. S. Lee, G. Bozoklu, W. Cai, S. T. Nguyen, R. S. Ruoff, *ACS Nano* **2008**, *2*, 572.

[72] S. Park, D. A. Dikin, S. T. Nguyen, R. S. Ruoff, *J. Phys. Chem. C* **2009**, *113*, 15801.

[73] P. Guo, H. H. Song, X. H. Chen, *Electrochem. Commun.* **2009**, *11*, 1320.

[74] H. Chen, M. B. Muller, K. J. Gilmore, G. G. Wallace, D. Li, *Adv. Mater.* **2008**, *20*, 3557.

[75] V. P. Gusynin, S. G. Sharapov, J. P. Carbotte, *Phys. Rev. Lett.* **2006**, *96*, 256802.

[76] N. M. R. Peres, *J. Phy. Condens. Matter* **2009**, *21*.

[77] R. R. Nair, P. Blake, A. N. Grigorenko, K. S. Novoselov, T. J. Booth, T. Stauber, N. M. R. Peres, A. K. Geim, *Science* **2008**, *320*, 1308.

[78] K. F. Mak, M. Y. Sfeir, Y. Wu, C. H. Lui, J. A. Misewich, T. F. Heinz, *Phys. Rev. Lett* **2008**, *101*, 196405.

[79] F. Wang, Y. B. Zhang, C. S. Tian, C. Girit, A. Zettl, M. Crommie, Y. R. Shen, *Science* **2008**, *320*, 206.

[80] P. A. George, J. Strait, J. Dawlaty, S. Shivaraman, M. Chandrashekhar, F. Rana, M. G. Spencer, *Nano Lett.* **2008**, *8*, 4248.

[81] F. Rana, P. A. George, J. H. Strait, J. Dawlaty, S. Shivaraman, M. Chandrashekhar, M. G. Spencer, *Phys. Rev. B* **2009**, *79*, 115447.

[82] F. Xia, T. Mueller, Y.-m. Lin, A. Valdes-Garcia, P. Avouris, *Nat. Nanotechnol.* **2009**, *4*, 839.

[83] P. Blake, E. W. Hill, A. H. C. Neto, K. S. Novoselov, D. Jiang, R. Yang, T. J. Booth, A. K. Geim, *Appl. Phys. Lett.* **2007**, *91*, 063124.

[84] Z. H. Ni, H. M. Wang, J. Kasim, H. M. Fan, T. Yu, Y. H. Wu, Y. P. Feng, Z. X. Shen, *Nano Lett.* **007**, *7*, 2758.

[85] S. Roddaro, P. Pingue, V. Piazza, V. Pellegrini, F. Beltram, *Nano Lett.* **2007**, *7*, 2707.

[86] I. Jung, M. Pelton, R. Piner, D. A. Dikin, S. Stankovich, S. Watcharotone, M. Hausner, R. S. Ruoff, *Nano Lett.* **2007**, *7*, 3569.

[87] D. S. L. Abergel, A. Russell, V. I. Fal'ko, *Appl. Phys. Lett.* **2007**, *91*, 063125.

[88] L. B. Gao, W. C. Ren, F. Li, H. M. Cheng, *ACS Nano* **2008**, *2*, 1625.

[89] C. Casiraghi, A. Hartschuh, E. Lidorikis, H. Qian, H. Harutyunyan, T. Gokus, K. S. Novoselov, A. C. Ferrari, *Nano Lett.* **2007**, *7*, 2711.

[90] V. Yu, M. Hilke, *Appl. Phys. Lett.* **2009**, *95*, 151904.

[91] *Handbook of Optical Constant of Solids*, Vol. 2, (Ed: E. D. Palik), Academic, New York **1991**.

[92] M. Bruna, S. Borini, *Appl. Phys. Lett.* **2009**, *94*, 031901.

[93] A. C. Ferrari, *Solid State Commun.* **2007**, *143*, 47.

[94] S. Piscanec, M. Lazzeri, F. Mauri, A. C. Ferrari, *Eur. Phys. J. Special Topics* **2007**, *148*, 159.

[95] Z. Ni, Y. Wang, T. Yu, Z. Shen, *Nano Research* **2008**, *1*, 273.

[96] L. M. Malard, M. A. Pimenta, G. Dresselhaus, M. S. Dresselhaus, *Phys. Rep.* **2009**, *473*, 51.

[97] A. C. Ferrari, J. C. Meyer, V. Scardaci, C. Casiraghi, M. Lazzeri, F. Mauri, S. Piscanec, D. Jiang, K. S. Novoselov, S. Roth, A. K. Geim, *Phys. Rev. Lett.* **2006**, *97*, 187401.

[98] J. Rohrl, M. Hundhausen, K. V. Emtsev, T. Seyller, R. Graupner, L. Ley, *Appl. Phys. Lett.* **2008**, *92*, 201918.

[99] Z. H. Ni, W. Chen, X. F. Fan, J. L. Kuo, T. Yu, A. T. S. Wee, Z. X. Shen, *Phys. Rev. B* **2008**, *77*, 115416.

[100] Y. Y. Wang, Z. H. Ni, T. Yu, Z. X. Shen, H. M. Wang, Y. H. Wu, W. Chen, A. T. S. Wee, *J. Phys. Chem. C* **2008**, *112*, 10637.

[101] J. Yan, Y. B. Zhang, P. Kim, A. Pinczuk, *Phys. Rev. Lett.* **2007**, *98*, 166802.

[102] S. Pisana, M. Lazzeri, C. Casiraghi, K. S. Novoselov, A. K. Geim, A. C. Ferrari, F. Mauri, *Nat. Mater.* **2007**, *6*, 198.

[103] J. A. Robinson, M. Wetherington, J. L. Tedesco, P. M. Campbell, X. Weng, J. Stitt, M. A. Fanton, E. Frantz, D. Snyder, B. L. VanMil, G. G. Jernigan, R. L. Myers-Ward, C. R. Eddy, D. K. Gaskill, *Nano Lett.* **2009**, *9*, 2873.

[104] C. Casiraghi, A. Hartschuh, H. Qian, S. Piscanec, C. Georgi, A. Fasoli, K. S. Novoselov, D. M. Basko, A. C. Ferrari, *Nano Lett.* **2009**, *9*, 1433.

[105] Y. M. You, Z. H. Ni, T. Yu, Z. X. Shen, *Appl. Phys. Lett.* **2008**, *93*, 163112.

[106] C. H. Yu, L. Shi, Z. Yao, D. Y. Li, A. Majumdar, *Nano Lett.* **2005**, *5*, 1842.

[107] S. Berber, Y. K. Kwon, D. Tomanek, *Phys. Rev. Lett.* **2000**, *84*, 4613.

[108] D. L. Nika, E. P. Pokatilov, A. S. Askerov, A. A. Balandin, *Phys. Rev. B* **2009**, *79*, 155413.

[109] Z. Guo, D. Zhang, X.-G. Gong, *Appl. Phys. Lett.* **2009**, *95*, 163103.

[110] S. Ghosh, I. Calizo, D. Teweldebrhan, E. P. Pokatilov, D. L. Nika, A. A. Balandin, W. Bao, F. Miao, C. N. Lau, *Appl. Phys. Lett.* **2008**, *92*.

[111] I. K. Hsu, M. T. Pows, A. Bushmaker, M. Aykol, L. Shi, S. B. Cronin, *Nano Lett.* **2009**, *9*, 590.

[112] I. Calizo, A. A. Balandin, W. Bao, F. Miao, C. N. Lau, *Nano Lett.* **2007**, *7*, 2645.

[113] W. Cai, A. L. Moore, Y. Zhu, X. Li, S. Chen, L. Shi, R. S. Ruoff, *Nano Lett.* **2010**, *10*, 1645.

[114] J. H. Seol, I. Jo, A. L. Moore, L. Lindsay, Z. H. Aitken, M. T. Pettes, X. Li, Z. Yao, R. Huang, D. Broido, N. Mingo, R. S. Ruoff, L. Shi, *Science* **2010**, *328*, 213.

[115] H. B. Heersche, P. Jarillo-Herrero, J. B. Oostinga, L. M. K. Vandersypen, A. F. Morpurgo, *Nature* **2007**, *446*, 56.

[116] M. P. Levendorf, C. S. Ruiz-Vargas, S. Garg, J. Park, *Nano Lett.* **2009**.

[117] Y. M. Lin, K. A. Jenkins, A. Valdes-Garcia, J. P. Small, D. B. Farmer, P. Avouris, *Nano Lett.* **2009**, *9*, 422.

[118] D. B. Farmer, H.-Y. Chiu, Y.-M. Lin, K. A. Jenkins, F. Xia, P. Avouris, *Nano Lett.* **2009**.

[119] Y.-M. Lin, C. Dimitrakopoulos, K. A. Jenkins, D. B. Farmer, H.-Y. Chiu, A. Grill, P. Avouris, *Science* **2010**, *327*, 662.

[120] L. A. Ponomarenko, F. Schedin, M. I. Katsnelson, R. Yang, E. W. Hill, K. S. Novoselov, A. K. Geim, *Science* **2008**, *320*, 356.

[121] S. Y. Zhou, G. H. Gweon, A. V. Fedorov, P. N. First, W. A. De Heer, D. H. Lee, F. Guinea, A. H. C. Neto, A. Lanzara, *Nat. Mater.* **2007**, *6*, 770.

[122] J. B. Oostinga, H. B. Heersche, X. L. Liu, A. F. Morpurgo, L. M. K. Vandersypen, *Nat. Mater.* **2008**, *7*, 151.

[123] Y. B. Zhang, T. T. Tang, C. Girit, Z. Hao, M. C. Martin, A. Zettl, M. F. Crommie, Y. R. Shen, F. Wang, *Nature* **2009**, *459*, 820.

[124] V. Barone, O. Hod, G. E. Scuseria, *Nano Lett.* **2006**, *6*, 2748.

[125] Y. W. Son, M. L. Cohen, S. G. Louie, *Phys. Rev. Lett.* **2006**, *97*, 216803.

[126] M. Y. Han, B. Ozyilmaz, Y. B. Zhang, P. Kim, *Phys. Rev. Lett.* **2007**, *98*, 206805.

[127] Z. Chen, Y.-M. Lin, M. J. Rooks, P. Avouris, *Phys. E* **2007**, *40*, 228.

[128] X. L. Li, X. R. Wang, L. Zhang, S. W. Lee, H. J. Dai, *Science* **2008**, *319*, 1229.

[129] L. Y. Jiao, L. Zhang, X. R. Wang, G. Diankov, H. J. Dai, *Nature* **2009**, *458*, 877.

[130] D. V. Kosynkin, A. L. Higginbotham, A. Sinitskii, J. R. Lomeda, A. Dimiev, B. K. Price, J. M. Tour, *Nature* **2009**, *458*, 872.

[131] J. R. Williams, L. DiCarlo, C. M. Marcus, *Science* **2007**, *317*, 638.

[132] D. A. Abanin, L. S. Levitov, *Science* **2007**, *317*, 641.

[133] V. V. Cheianov, V. Fal'ko, B. L. Altshuler, *Science* **2007**, *315*, 1252.

[134] G. Liu, J. Velasco, W. Z. Bao, C. N. Lau, *Appl. Phys. Lett.* **2008**, *92*, 203103.

[135] X. R. Wang, X. L. Li, L. Zhang, Y. Yoon, P. K. Weber, H. L. Wang, J. Guo, H. J. Dai, *Science* **2009**, *324*, 768.

[136] X. Li, H. Wang, J. T. Robinson, H. Sanchez, G. Diankov, H. Dai, *J. Am. Chem. Soc.* **2009**.

[137] A. Das, S. Pisana, B. Chakraborty, S. Piscanec, S. K. Saha, U. V. Waghmare, K. S. Novoselov, H. R. Krishnamurthy, A. K. Geim, A. C. Ferrari, A. K. Sood, *Nat. Nanotechnol.* **2008**, *3*, 210.

[138] W. Chen, S. Chen, D. C. Qi, X. Y. Gao, A. T. S. Wee, *J. Am. Chem. Soc.* **2007**, *129*, 10418.

[139] Y. P. Dan, Y. Lu, N. J. Kybert, Z. T. Luo, A. T. C. Johnson, *Nano Lett.* **2009**, *9*, 1472.

[140] J. T. Robinson, F. K. Perkins, E. S. Snow, Z. Q. Wei, P. E. Sheehan, *Nano Lett.* **2008**, *8*, 3137.

[141] L. H. Tang, Y. Wang, Y. M. Li, H. B. Feng, J. Lu, J. H. Li, *Adv. Funct. Mater.* **2009**, *19*, 2782.

[142] Y. Ohno, K. Maehashi, Y. Yamashiro, K. Matsumoto, *Nano Lett.* **2009**, *9*, 3318.

[143] N. Mohanty, V. Berry, *Nano Lett.* **2008**, *8*, 4469.

[144] B. Huang, Z. Y. Li, Z. R. Liu, G. Zhou, S. G. Hao, J. Wu, B. L. Gu, W. H. Duan, *J. Phys. Chem. C* **2008**, *112*, 13442.

[145] T. O. Wehling, K. S. Novoselov, S. V. Morozov, E. E. Vdovin, M. I. Katsnelson, A. K. Geim, A. I. Lichtenstein, *Nano Lett.* **2008**, *8*, 173.

[146] O. Leenaerts, B. Partoens, F. M. Peeters, *Phys. Rev. B* **2008**, *77*, 125416.

[147] W. W. Cai, D. Chen, X. S. Li, Y. W. Zhu, D. R. Piner, R. S. Ruoff, *unpublished*.

[148] H. A. Becerril, J. Mao, Z. Liu, R. M. Stoltenberg, Z. Bao, Y. Chen, *ACS Nano* **2008**, *2*, 463.

[149] X. Wang, L. J. Zhi, K. Mullen, *Nano Lett.* **2008**, *8*, 323.

[150] G. Eda, G. Fanchini, M. Chhowalla, *Nat. Nanotechnol.* **2008**, *3*, 270.

[151] L. J. Cote, F. Kim, J. X. Huang, *J. Am. Chem. Soc.* **2009**, *131*, 1043.

[152] S. Park, R. S. Ruoff, *Nat. Nanotechnol.* **2009**, *4*, 217.

[153] D. Li, M. B. Muller, S. Gilje, R. B. Kaner, G. G. Wallace, *Nat. Nanotechnol.* **2008**, *3*, 101.

[154] X. L. Li, G. Y. Zhang, X. D. Bai, X. M. Sun, X. R. Wang, E. Wang, H. J. Dai, *Nat. Nanotechnol.* **2008**, *3*, 538.

[155] S. Biswas, L. T. Drzal, *Nano Lett.* **2009**, *9*, 167.

[156] Y. Hernandez, V. Nicolosi, M. Lotya, F. M. Blighe, Z. Y. Sun, S. De, I. T. McGovern, B. Holland, M. Byrne, Y. K. Gun'ko, J. J. Boland, P. Niraj, G. Duesberg, S. Krishnamurthy, R. Goodhue, J. Hutchison, V. Scardaci, A. C. Ferrari, J. N. Coleman, *Nat. Nanotechnol.* **2008**, *3*, 563.

[157] S. De, P. J. King, M. Lotya, A. O'Neill, E. M. Doherty, Y. Hernandez, G. S. Duesberg, J. N. Coleman, *Small* **2009**, *6*, 458.

[158] Y. Zhu, W. Cai, R. D. Piner, A. Velamakanni, R. S. Ruoff, *Appl. Phys. Lett.* **2009**, *95*, 103104.

[159] P. Blake, P. D. Brimicombe, R. R. Nair, T. J. Booth, D. Jiang, F. Schedin, L. A. Ponomarenko, S. V. Morozov, H. F. Gleeson, E. W. Hill, A. K. Geim, K. S. Novoselov, *Nano Lett.* **2008**, *8*, 1704.

[160] J. Wu, M. Agrawal, H. A. Becerril, Z. Bao, Z. Liu, Y. Chen, P. Peumans, *ACS Nano* **2009**, *4*, 43.

[161] K. S. Kim, Y. Zhao, H. Jang, S. Y. Lee, J. M. Kim, K. S. Kim, J. H. Ahn, P. Kim, J. Y. Choi, B. H. Hong, *Nature* **2009**, *457*, 706.

[162] A. Reina, X. T. Jia, J. Ho, D. Nezich, H. B. Son, V. Bulovic, M. S. Dresselhaus, J. Kong, *Nano Lett.* **2009**, *9*, 3087.

[163] J. H. Chen, C. Jang, S. D. Xiao, M. Ishigami, M. S. Fuhrer, *Nat. Nanotechnol.* **2008**, *3*, 206.

[164] M. Winter, J. O. Besenhard, M. E. Spahr, P. Novak, *Adv. Mater.* **1998**, *10*, 725.

[165] Y. H. Liu, J. S. Xue, T. Zheng, J. R. Dahn, *Carbon* **1996**, *34*, 193.

[166] E. Yoo, J. Kim, E. Hosono, H. Zhou, T. Kudo, I. Honma, *Nano Lett.* **2008**, *8*, 2277.

[167] D. Y. Pan, S. Wang, B. Zhao, M. H. Wu, H. J. Zhang, Y. Wang, Z. Jiao, *Chem. Mat.* **2009**, *21*, 3136.

[168] C. Y. Wang, D. Li, C. O. Too, G. G. Wallace, *Chem. Mat.* **2009**, *21*, 2604.

[169] J. K. Lee, K. B. Smith, C. M. Hayner, H. H. Kung, *Chem. Commun.* **2010**, *46*, 2025.

[170] M. H. Liang, L. J. Zhi, *J. Mater. Chem.* **2009**, *19*, 5871.

[171] N. A. Kaskhedikar, J. Maier, *Adv. Mater.* **2009**, *21*, 2664.

[172] J. Yao, X. Shen, B. Wang, H. Liu, G. Wang, *Electrochem. Commun.* **2009**, *11*, 1849.

[173] S. M. Paek, E. Yoo, I. Honma, *Nano Lett.* **2009**, *9*, 72.

[174] D. H. Wang, D. W. Choi, J. Li, Z. G. Yang, Z. M. Nie, R. Kou, D. H. Hu, C. M. Wang, L. V. Saraf, J. G. Zhang, I. A. Aksay, J. Liu, *ACS Nano* **2009**, *3*, 907.

[175] C. Xu, X. Wang, L. Yang, Y. Wu, *J. Solid State Chem.* **2009**, *182*, 2486.

[176] S. Yang, G. Cui, S. Pang, Q. Cao, U. Kolb, X. Feng, J. Maier, K. Müllen, *ChemSusChem* **2009**, *3*, 236.

[177] G. Wang, B. Wang, X. Wang, J. Park, S. Dou, H. Ahn, K. Kim, *J. Mater. Chem.* **2009**, *19*, 8378.

[178] B. E. Conway, *Electrochemical Supercapacitors: Scientific Fundamentals and Technological Applications*, Plenum Publishers, New York **1999**.

[179] P. Simon, Y. Gogotsi, *Nat Mater* **2008**, *7*, 845.

[180] M. D. Stoller, S. J. Park, Y. W. Zhu, J. H. An, R. S. Ruoff, *Nano Lett.* **2008**, *8*, 3498.

[181] Y. Wang, Z. Shi, Y. Huang, Y. Ma, C. Wang, M. Chen, Y. Chen, *J. Phys. Chem. C* **2009**, *113*, 13103.

[182] Y. Zhu, S. Murali, M. D. Stoller, A. Velamakanni, R. D. Piner, R. S. Ruoff, *Carbon* **2010**, *48*, 2118.

[183] Y. Zhu, M. D. Stoller, W. Cai, A. Velamakanni, R. D. Piner, D. Chen, R. S. Ruoff, *ACS Nano* **2010**, *4*, 1227.

[184] S. R. C. Vivekchand, C. S. Rout, K. S. Subrahmanyam, A. Govindaraj, C. N. R. Rao, *J. Chem. Sci.* **2008**, *120*, 9.

[185] W. Lv, D.-M. Tang, Y.-B. He, C.-H. You, Z.-Q. Shi, X.-C. Chen, C.-M. Chen, P.-X. Hou, C. Liu, Q.-H. Yang, *ACS Nano* **2009**, *3*, 3730.

[186] Y. C. Si, E. T. Samulski, *Chem. Mater.* **2008**, *20*, 6792.

[187] Y. P. Zhang, H. B. Li, L. K. Pan, T. Lu, Z. Sun, *J. Electroanal. Chem.* **2009**, *634*, 68.

[188] F. H. Li, J. F. Song, H. F. Yang, S. Y. Gan, Q. X. Zhang, D. X. Han, A. Ivaska, L. Niu, *Nanotechnology* **2009**, *20*, 6.

[189] S. Chen, J. Zhu, X. Wu, Q. Han, X. Wang, *ACS Nano* **2010**, *4*, 2822.

[190] D. Yu, L. Dai, *J. Phys. Chem. Lett.* **2009**, *1*, 467.

[191] D.-W. Wang, F. Li, J. Zhao, W. Ren, Z.-G. Chen, J. Tan, Z.-S. Wu, I. Gentle, G. Q. Lu, H.-M. Cheng, *ACS Nano* **2009**, *3*, 1745.

[192] A. V. Murugan, T. Muraliganth, A. Manthiram, *Chem. Mat.* **2009**, *21*, 5004.

[193] H. L. Wang, Q. L. Hao, X. J. Yang, L. D. Lu, X. Wang, *Electrochem. Commun.* **2009**, *11*, 1158.

[194] Q. Wu, Y. Xu, Z. Yao, A. Liu, G. Shi, *Acs Nano* **2010**, *4*, 1963.

[195] G. Srinivas, Y. Zhu, R. Piner, N. Skipper, M. Ellerby, R. Ruoff, *Carbon* **2009**, *48*, 630.

[196] Y. Li, L. Tang, J. Li, *Electrochem. Commun.* **2009**, *11*, 846.

[197] B. Seger, P. V. Kamat, *J. Phys. Chem. C* **2009**, *113*, 7990.

[198] C. Xu, X. Wang, J. Zhu, *J. Phys. Chem. C* **2008**, *112*, 19841.

[199] E. Yoo, T. Okata, T. Akita, M. Kohyama, J. Nakamura, I. Honma, *Nano Lett.* **2009**, *9*, 2255.

[200] R. Kou, Y. Shao, D. Wang, M. H. Engelhard, J. H. Kwak, J. Wang, V. V. Viswanathan, C. Wang, Y. Lin, Y. Wang, I. A. Aksay, J. Liu, *Electrochem. Commun.* **2009**, *11*, 954.

[201] G. Eda, Y.-Y. Lin, S. Miller, C.-W. Chen, W.-F. Su, M. Chhowalla, *Appl. Phys. Lett.* **2008**, *92*, 233305.

[202] J. Wu, H. A. Becerril, Z. Bao, Z. Liu, Y. Chen, P. Peumans, *Appl. Phys. Lett.* **2008**, *92*, 263302.

[203] W. Hong, Y. Xu, G. Lu, C. Li, G. Shi, *Electrochem. Comm.* **2008**, *10*, 1555.

[204] B. Z. Jang, A. Zhamu, *J. Mater. Sci.* **2008**, *43*, 5092.

[205] M. Fang, K. G. Wang, H. B. Lu, Y. L. Yang, S. Nutt, *J. Mater. Chem.* **2009**, *19*, 7098.

[206] H. Hu, X. Wang, J. Wang, L. Wan, F. Liu, H. Zheng, R. Chen, C. Xu, *Chemical Physics Letters* **2010**, *484*, 247.

[207] S. H. Lee, D. R. Dreyer, J. An, A. Velamakanni, R. D. Piner, S. Park, Y. Zhu, S. O. Kim, C. W. Bielawski, R. S. Ruoff, *Macromol. Rapid Comm.* **2009**, *30*.

[208] T. Ramanathan, A. A. Abdala, S. Stankovich, D. A. Dikin, M. Herrera-Alonso, R. D. Piner, D. H. Adamson, H. C. Schniepp, X. Chen, R. S. Ruoff, S. T. Nguyen, I. A. Aksay, R. K. Prud'homme, L. C. Brinson, *Nat. Nanotechnol.* **2008**, *3*, 327.

[209] J. J. Liang, Y. Huang, L. Zhang, Y. Wang, Y. F. Ma, T. Y. Guo, Y. S. Chen, *Adv. Funct. Mater.* **2009**, *19*, 2297.

[210] H. J. Salavagione, G. Martinez, M. A. Gomez, *J. Mater. Chem.* **2009**, *19*, 5027.

[211] J. H. Wu, Q. W. Tang, H. Sun, J. M. Lin, H. Y. Ao, M. L. Huang, Y. F. Huang, *Langmuir* **2008**, *24*, 4800.

[212] K. Kalaitzidou, H. Fukushima, L. T. Drzal, *Compos. Sci. Technol.* **2007**, *67*, 2045.

[213] K. Wakabayashi, C. Pierre, D. A. Dikin, R. S. Ruoff, T. Ramanathan, L. C. Brinson, J. M. Torkelson, *Macromolecules* **2008**, *41*, 1905.

[214] S. Ganguli, A. K. Roy, D. P. Anderson, *Carbon* **2008**, *46*, 806.

[215] M. A. Rafiee, J. Rafiee, Z. Z. Yu, N. Koratkar, *Appl. Phys. Lett.* **2009**, *95*, 3.

[216] S. R. Wang, M. Tambraparni, J. J. Qiu, J. Tipton, D. Dean, *Macromolecules* **2009**, *42*, 5251.

[217] A. P. Yu, P. Ramesh, M. E. Itkis, E. Bekyarova, R. C. Haddon, *J. Phys. Chem. C* **2007**, *111*, 7565.

[218] H. Kim, C. W. Macosko, *Macromolecules* **2008**, *41*, 3317.

[219] R. Verdejo, F. Barroso-Bujans, M. A. Rodriguez-Perez, J. A. de Saja, M. A. Lopez-Manchado, *J. Mater. Chem.* **2008**, *18*, 2221.

[220] D. Cai, K. Yusoh, M. Song, *Nanotechnology* **2009**, *20*, 5.

[221] Y. R. Lee, A. V. Raghu, H. M. Jeong, B. K. Kim, *Macromol. Chem. Phys.* **2009**, *210*, 1247.

[222] S. Ansari, E. P. Giannelis, *J. Pol. Sci., Part B Polym. Phys.* **2009**, *47*, 888.

[223] H. Kim, C. W. Macosko, *Polymer* **2009**, *50*, 3797.

[224] E. T. Thostenson, C. Y. Li, T. W. Chou, *Compos. Sci. Technol.* **2005**, *65*, 491.

[225] M. J. McAllister, J.-L. Li, D. H. Adamson, H. C. Schniepp, A. A. Abdala, J. Liu, M. Herrera-Alonso, D. L. Milius, R. Car, R. K. Prud'homme, I. A. Aksay, *Chem. Mat.* **2007**, *19*, 4396.

[226] P. Steurer, R. Wissert, R. Thomann, R. Mulhaupt, *Macromol. Rapid Commun.* **2009**, *30*, 316.

[227] L. M. Veca, F. S. Lu, M. J. Meziani, L. Cao, P. Y. Zhang, G. Qi, L. W. Qu, M. Shrestha, Y. P. Sun, *Chem. Commun.* **2009**, 2565.

[228] Y. F. Yang, J. Wang, J. Zhang, J. C. Liu, X. L. Yang, H. Y. Zhao, *Langmuir* **2009**, *25*, 11808.

[229] T. Wei, G. L. Luo, Z. J. Fan, C. Zheng, J. Yan, C. Z. Yao, W. F. Li, C. Zhang, *Carbon* **2009**, *47*, 2296.

[230] X. S. Du, Z. Z. Yu, A. Dasari, J. Ma, M. S. Mo, Y. Z. Meng, Y. W. Mai, *Chem. Mater.* **2008**, *20*, 2066.

[231] J. L. Vickery, A. J. Patil, S. Mann, *Adv. Mater.* **2009**, *21*, 2180.

[232] J. W. May, *Surf. Sci.* **1969**, *17*, 267.

[233] J. C. Shelton, H. R. Patil, J. M. Blakely, *Surf. Sci.* **1974**, *43*, 493.

[234] M. Eizenberg, J. M. Blakely, *J. Chem. Phys.* **1979**, *71*, 3467.

[235] M. Eizenberg, J. M. Blakely, *Surf. Sci.* **1979**, *82*, 228.

[236] J. C. Hamilton, J. M. Blakely, *Surf. Sci.* **1980**, *91*, 119.

[237] C. Berger, Z. Song, X. Li, X. Wu, N. Brown, C. Naud, D. Mayou, T. Li, J. Hass, a. A. N. Marchenkov, E. H. Conrad, P. N. First, W. A. de Heer, *Science* **2006**, *312*, 1991.

[238] W. A. de Heer, C. Berger, X. Wu, P. N. First, E. H. Conrad, X. Li, T. Li, M. Sprinkle, J. Hass, M. L. Sadowski, M. Potemski, G. Martinez, *Solid State Commun.* **2007**, *143*, 92.

[239] K. V. Emtsev, A. Bostwick, K. Horn, J. Jobst, G. L. Kellogg, L. Ley, J. L. McChesney, T. Ohta, S. A. Reshanov, J. Rohrl, E. Rotenberg, A. K. Schmid, D. Waldmann, H. B. Weber, T. Seyller, *Nat. Mater.* **2009**, *8*, 203.

[240] H. Huang, W. Chen, S. Chen, A. T. S. Wee, *ACS Nano* **2008**, *2*, 2513.

[241] X. S. Li, W. W. Cai, L. Colombo, R. S. Ruoff, *Nano Lett.* **2009**, *9*, 4268.

[242] Y. B. Zhang, J. P. Small, W. V. Pontius, P. Kim, *Appl. Phys. Lett.* **2005**, *86*, 3.

[243] H. P. Boehm, A. Clauss, G. Fischer, U. Hofmann, "Surface properties of extremely thin graphite lamellae", presented at *the Fifth Conference on Carbon*, **1962**.

[244] A. Dato, V. Radmilovic, Z. H. Lee, J. Phillips, M. Frenklach, *Nano Lett.* **2008**, *8*, 2012.

[245] N. Li, Z. Wang, K. Zhao, Z. Shi, Z. Gu, S. Xu, *Carbon* **2010**, *48*, 255.

[246] Q. K. Yu, J. Lian, S. Siriponglert, H. Li, Y. P. Chen, S. S. Pei, *Appl. Phys. Lett.* **2008**, *93*, 113103.

[247] L. Staudenmaier, *Ber. Deut. Chem. Ges.* **1898**, *31*, 1481.

[248] W. S. Hummers, R. E. Offeman, *J. Am. Chem. Soc.* **1958**, *80*, 1339.

[249] H. P. Boehm, M. Eckel, W. Scholz, *Z. Anorg. Allgem. Chem.* **1967**, *353*, 236.

[250] W. W. Cai, R. D. Piner, F. J. Stadermann, S. Park, M. A. Shaibat, Y. Ishii, D. X. Yang, A. Velamakanni, S. J. An, M. Stoller, J. H. An, D. M. Chen, R. S. Ruoff, *Science* **2008**, *321*, 1815.

[251] J. I. Paredes, S. Villar-Rodil, A. Martinez-Alonso, J. M. D. Tascon, *Langmuir* **2008**, *24*, 10560.

[252] S. Stankovich, D. A. Dikin, R. D. Piner, K. A. Kohlhaas, A. Kleinhammes, Y. Jia, Y. Wu, S. T. Nguyen, R. S. Ruoff, *Carbon* **2007**, *45*, 1558.

[253] G. X. Wang, J. Yang, J. Park, X. L. Gou, B. Wang, H. Liu, J. Yao, *J. Phys. Chem. C* **2008**, *112*, 8192.

[254] Y. Si, E. T. Samulski, *Nano Lett.* **2008**, *8*, 1679.

[255] H.-J. Shin, K. K. Kim, A. Benayad, S.-M. Yoon, H. K. Park, I.-S. Jung, M. H. Jin, H.-K. Jeong, J. M. Kim, J.-Y. Choi, Y. H. Lee, *Adv. Funct. Mater.* **2009**, *19*, 1987.

[256] V. Dua, S. P. Surwade, S. Ammu, S. R. Agnihotra, S. Jain, K. E. Roberts, S. Park, R. S. Ruoff, S. K. Manohar, *Angew. Chem. Int. Ed.* **2010**, *122*, 2200.

[257] H. C. Schniepp, J.-L. Li, M. J. McAllister, H. Sai, M. Herrera-Alonso, D. H. Adamson, R. K. Prud'homme, R. Car, D. A. Saville, I. A. Aksay, *J. Phys. Chem. B* **2006**, *110*, 8535.

[258] M. Zhou, Y. L. Wang, Y. M. Zhai, J. F. Zhai, W. Ren, F. A. Wang, S. J. Dong, *Chem. Eur. J.* **2009**, *15*, 6116.

[259] W. Gao, L. B. Alemany, L. Ci, P. M. Ajayan, *Nat. Chem.* **2009**, *1*, 403.

[260] S. J. An, Y. Zhu, S. H. Lee, M. D. Stoller, T. Emilsson, S. Park, A. Velamakanni, J. Ho, R. S. Ruoff, *J. Phys. Chem. Lett.* **2010**, *1*, 1259.